CHAPTER 3

TOWARDS MULTI-STATION ROTAXANES AND CATENANES USING METALLOPORPHYRIN COORDINATION TEMPLATING

3.1 INTRODUCTION

In Chapter 1, we discussed the notion of multi-station supramolecular systems capable of controlled motion. To this end, multiple functionalities have been incorporated into rotaxanes and catenanes, and examples of "switching" between the various sites *via* chemical[1], electrochemical[2, 3] and photochemical[3-5] means have been reported.

As the complexity of these systems increases, efficient templating to achieve reasonable yields during their synthesis becomes crucial. Thus we have become interested in using rhodium and ruthenium strapped porphyrins as effective templates for a new range of catenanes and rotaxanes. In this design, we intend to use the templating effect resulting from strong coordination of an appropriately substituted pyridine-based component to produce non-symmetrical dual functionalised catenanes or multi-station rotaxanes which can be addressed or driven by several different stimuli or inputs (see Scheme 3.1).

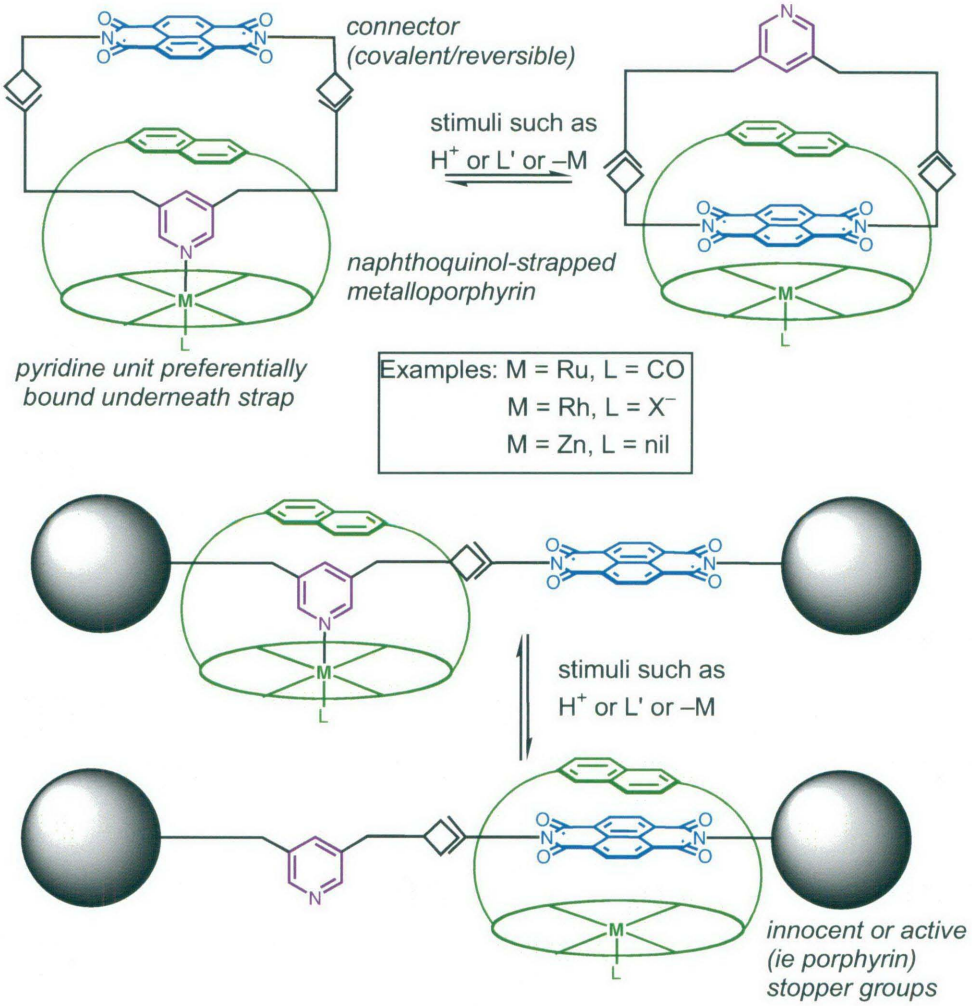

Scheme 3.1:- Schematic illustrating templated catenane formation utilizing strong pyridine/metalloporphyrin coordination, and a neutral naphthodiimide unit. The pyridine unit must be bound preferentially underneath the strap for effective templating. Protonation of the pyridine, addition of exogenous competing ligand L' or removal of the metal ion are several of many factors that can be used to reversibly 'drive' the catenane, causing rotation of the entrapped macrocycle. Similar concepts relying on the templating ability of an appropriately functionalised pyridine can be used to assemble multi-station rotaxanes with a variety of 'innocent' or 'active' (eg porphyrin) stopper groups.

The components that can be utilised in such a scheme, that were thus chosen for investigation can be seen in Figure 3.1.

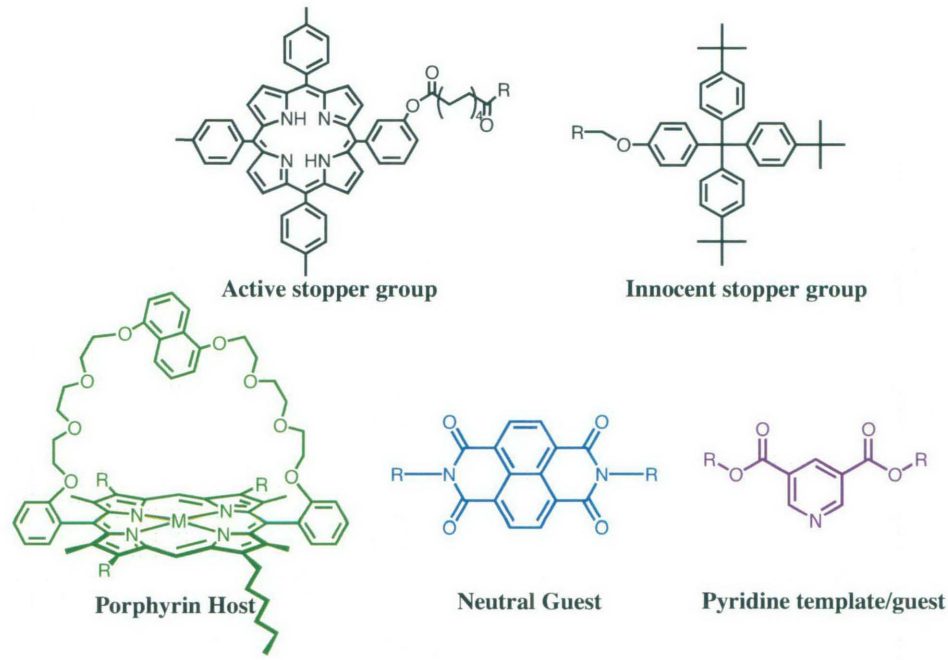

Figure 3.1:- Components used in this study.

3.2 PRELIMINARY STUDIES

Although we had shown that the difunctionalised pyridine esters such as those shown in Figure 3.1 were only relatively weak ligands for zinc porphyrins (see Chapter 2), this *per se* did not rule them out as possible candidates for templated assembly of rotaxanes and catenanes. Reaction conditions that favoured coordination (low temperatures, non-competitive solvents, high concentrations etc.) may well produce the desired outcomes. Alternatively, the incorporation of a diimide moiety as a possible second station could also act as the templating moiety producing interlocked species, as had been shown previously in the successful production of diimide based porphyrin catenanes.[4, 6] Thus the synthesis of catenane **3.4** was attempted using an EDC (1-(3-dimethylaminopropyl)-3-ethylcarbodiimide hydrochloride) promoted condensation reaction between diimide **3.1** and the pyridine ligand **3.3** in the presence of zinc strapped porphyrin **3.2** as outlined in Scheme 3.2.

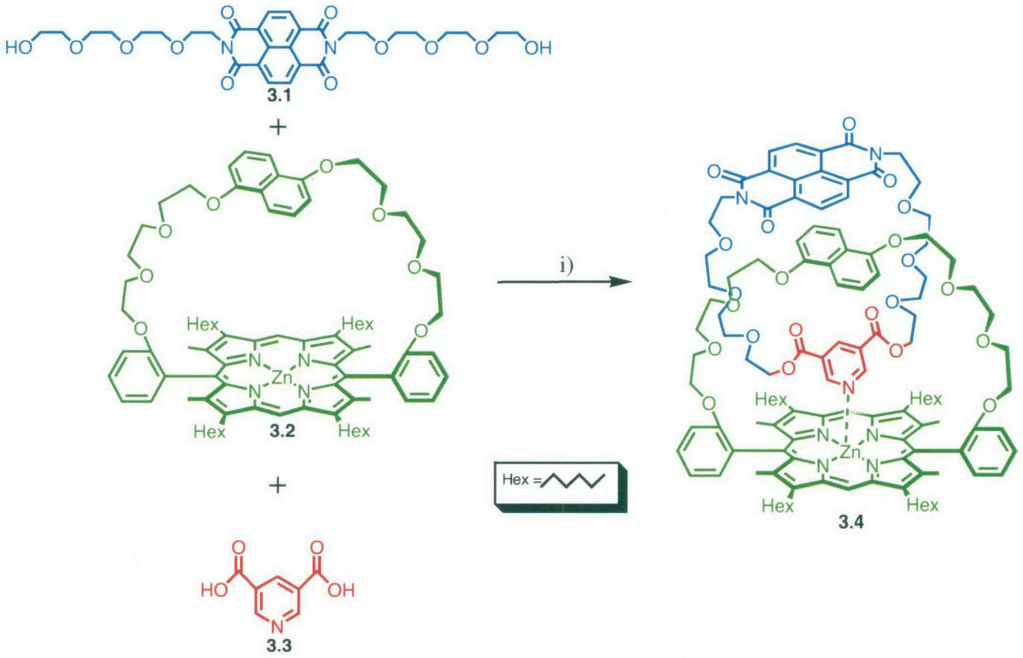

Scheme 3.2:- Reagents and conditions for the synthesis of catenane **3.4**; i) EDC, dry DMF, 6 days RT.

Subsequent workup of the reaction mixture showed that the reactants **3.1** and **3.3** had been consumed, however 95% of starting material **3.2** was recovered and only trace amounts of other porphyrinic material was detected, none of which could be identified as catenane. Thus it was deemed that in this case the weak coordination of the pyridine was not sufficient to template the reaction and yield any substantial amounts of catenane. Any future attempts would need to involve a stronger coordinating metal-ligand interaction. For the same pyridine-based ligands, this implied a stronger Lewis acid metalloporphyrin. Possible candidates which are known to exhibit substantially enhanced binding of pyridine ligands are the corresponding ruthenium and rhodium derivatives of the same strapped porphyrins, as discussed in Chapter 2.

3.3 CATENANE ATTEMPTS USING RhCl STRAPPED PORPHYRIN AND PYRIDINE TEMPLATES

As discussed in Chapter 2, one of the problems with using ruthenium or rhodium strapped porphyrins, and the particular 3,5-disubstituted pyridine ligand chosen for this investigation, is the tendency of the ligand to migrate to the "outside" position of the strapped porphyrin rather than bind underneath the strap of the porphyrin. A suitable

strapped porphyrin host was determined to be the rhodium chloride porphyrin derivative **3.5** (see Figure 3.2), as "inside" coordination of the pyridine ligand was observed initially, and this geometry was shown to be relatively stable with only 20% conversion to the "outside" face of the porphyrin after three days at room temperature in the weakly coordinating solvent $CDCl_3$. Thus in designing a synthetic route to catenanes using this porphyrin/ligand combination, the choice of reaction conditions is critical; optimal conditions which would minimise ligand migration would be reactions at room temperature (or below) in non-coordinating solvents such as DCM, and those with fast kinetic pathways.

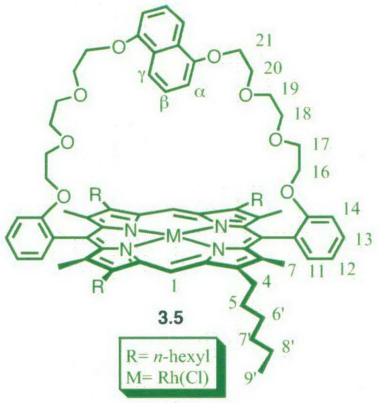

Figure 3.2:- Strapped porphyrin used in future attempts for catenane and rotaxane synthesis.

Two mild and reagent compatible synthetic methods to produce two-station catenanes were initially considered, firstly a Mitsunobu reaction between pyridine **3.6** and naphthalene diimide **3.7**, and secondly a repeat of the initial catenane attempt using an EDC condensation between pyridine diacid **3.3** and the diimide thread unit **3.1** as discussed in Section 3.2, however replacing the zinc porphyrin **3.2** with the rhodium porphyrin **3.5** (see Scheme 3.3 and 3.2 respectively).

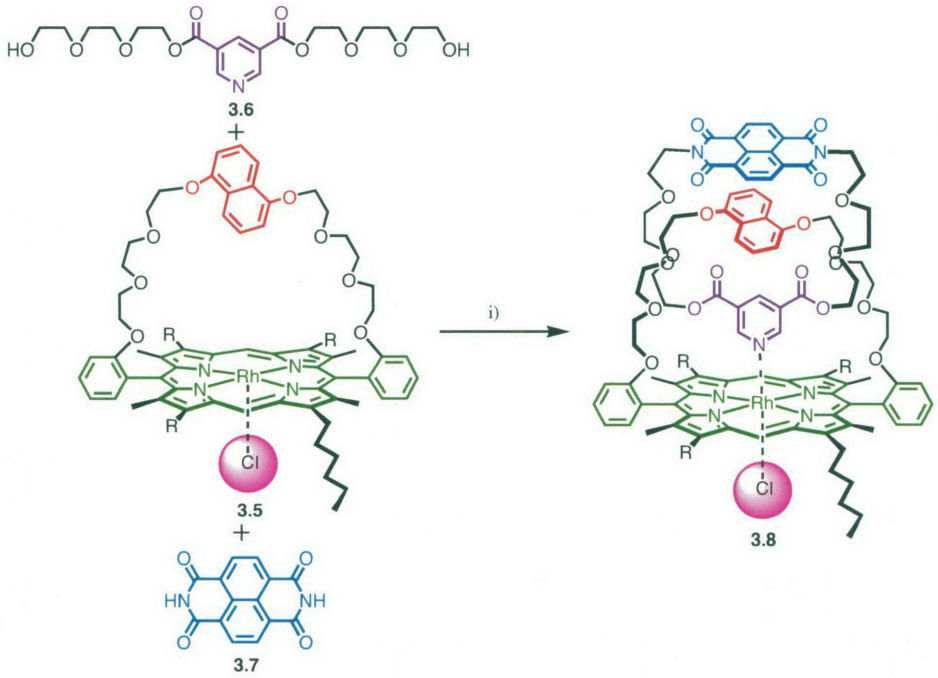

Scheme 3.3:- Reagents and conditions for the synthesis of catenane **3.8**; i) DEAD, PPh_3, dry THF, 16 h RT.

The Mitsunobu reaction seemed ideal as reaction times are typically short (12-24 hours) at ambient temperatures, and catenanes incorporating diimides have been previously synthesised using this method.[7] However in our case, no catenane was isolated, and furthermore, it was found that the starting porphyrin material had been degraded to an unidentifiable mixture. Attempts to determine the cause of this proved unsuccessful, in that addition of each of the reagents separately to the strapped porphyrin showed no obvious decomposition. Presumably either a reaction intermediate or a side product produced during the reaction is responsible for degradation of the starting material, but this was not investigated further.*

The alternative EDC condensation reactions showed promise as they can be performed at room temperature, but the longer reaction times (typically 1-7 days) may be troublesome. Another immediate concern was that the pyridine diacid **3.3** was insoluble in typical non-coordinating solvents such as DCM. An alternative solvent such as DMF in which the ligand is soluble, may compete for coordination to the rhodium porphyrin and thus

* These reagents have been used in the synthesis of catenanes incorporating similar crown ether-diimide moieties without any degradation observed. Therefore it is assumed that the Mitsunobu reagents must be degrading either the porphyrin ring or pyridine ligand and not the crown ether strap or diimide moieties.

negating any templating effect of the pyridine. Reactions in non-coordinating solvents such as DCM however are also problematic, as slower reaction times due to insolubility of the pyridine diacid may reduce the chance of catenation due to the competing slow ligand migration to the outside of the porphyrin face. Nevertheless EDC condensations using both dry DMF and dry DCM were attempted.[†]

Workup of both of the reaction mixtures carried out in the different solvents showed multiple porphyrin components, none of which were identified as catenane. The primary porphyrin component that could be separated by preparative thin layer chromatography was in fact determined to be a mixture of the diimide starting material and triethylamine-coordinated strapped porphyrin.[‡] In the ^{1}H NMR spectrum of the mixture, the bound triethylamine appeared as a triplet at –2.56 and a quartet at –2.15 ppm; however other peaks were also apparent at –0.40, and –1.25 ppm. To confirm that these upfield peaks were due to bound triethylamine, control experiments were performed by addition of one equivalent of triethylamine to a pure sample of the strapped porphyrin **3.5**. The addition of triethylamine initially resulted in the appearance of four multiplets at –0.40, –1.25, –2.12 and –2.56. Apart from very minor chemical shift differences which could be due to concentration or subtle effects of the other components in the reaction mixture, these are consistent with the peaks observed in the catenation attempt, thus confirming the identity of the porphyrin component of the major spot. The multiple sets of peaks might indicate the presence of both "inside" and "outside" coordinated triethylamine. Indeed over time the more downfield pair decreased in intensity relative to the more upfield pair of protons. This could be evidence of exchange from outside to inside coordination of triethylamine as seen with some pyridine ligands in Chapter 2, although this aspect was not pursued further here.

[†] Although it is common to add HOBT (1-Hydroxybenzotriazole hydrate) to EDC reactions as a catalyst, this was not included in any of our catenane attempts using metallated porphyrins as the HOBT has previously been found to coordinate to the metal in the porphyrin, and in this case would be a potential competing ligand for the pyridine diacid template.

[‡] Because of the exceptionally strong binding of nitrogenous ligands to rhodium porphyrins, in our experience it is not unusual for the intact complexes to survive chromatographic separation, even when using potentially competing polar solvents such as methanol.

Further investigation into the possible identity of the other porphyrin spots revealed that the EDC reagent itself produced multiple porphyrin spots on a TLC plate, when added to a solution of rhodium strapped porphyrin. This indicated that the EDC was binding to or reacting with the rhodium strapped porphyrin and hence was not an ideal reagent as it too could compete with the pyridine ligand for complexation. Nevertheless it should be noted that both triethylamine and EDC are not usually problematic in zinc porphyrin reactions, and so the difficulties in this case are presumably a direct result of the stronger complexing ability and/or reactivity of the rhodium derivatives.

Attempts to repeat the same reaction in the absence of triethylamine and using the reagent DCC (*N,N'*-Dicyclohexylcarbodiimide), which lacks the potentially coordinating tertiary amine group of EDC, were undertaken. However unfortunately even after 7 days at room temperature no reaction was detected. It was presumed that without the use of HOBT or triethylamine, the DCC could not react in a timely fashion and although it may react with heat and more time, these conditions are not conducive to catenane formation due to the tendency for the ligand to migrate to the outside under such conditions. Thus it appeared that this type of reaction was unsuitable for producing catenanes using the pyridine **3.3** and the porphyrin **3.5** and alternative synthetic strategies were needed.

3.4 ROTAXANES *VIA* ESTER FORMATION

Another synthetic scheme that would provide both short reaction times and room temperature conditions, key factors in ensuring inside coordination of these pyridine templates, is the use of acid chloride reactions. It was envisioned that in the first instance simple rotaxanes assembled by pyridine templates could be synthesised by reaction between pyridine ligand **3.6** and mono-sebacoyloxy tetratolyl porphyrin **3.9**. For further simplicity, a mono-substituted porphyrin pyridine thread **3.11** with one end already stoppered was synthesised *via* an EDC reaction between pyridine diol **3.6** and the same sebacoyl porphyrin **3.9** (see Scheme 3.4).

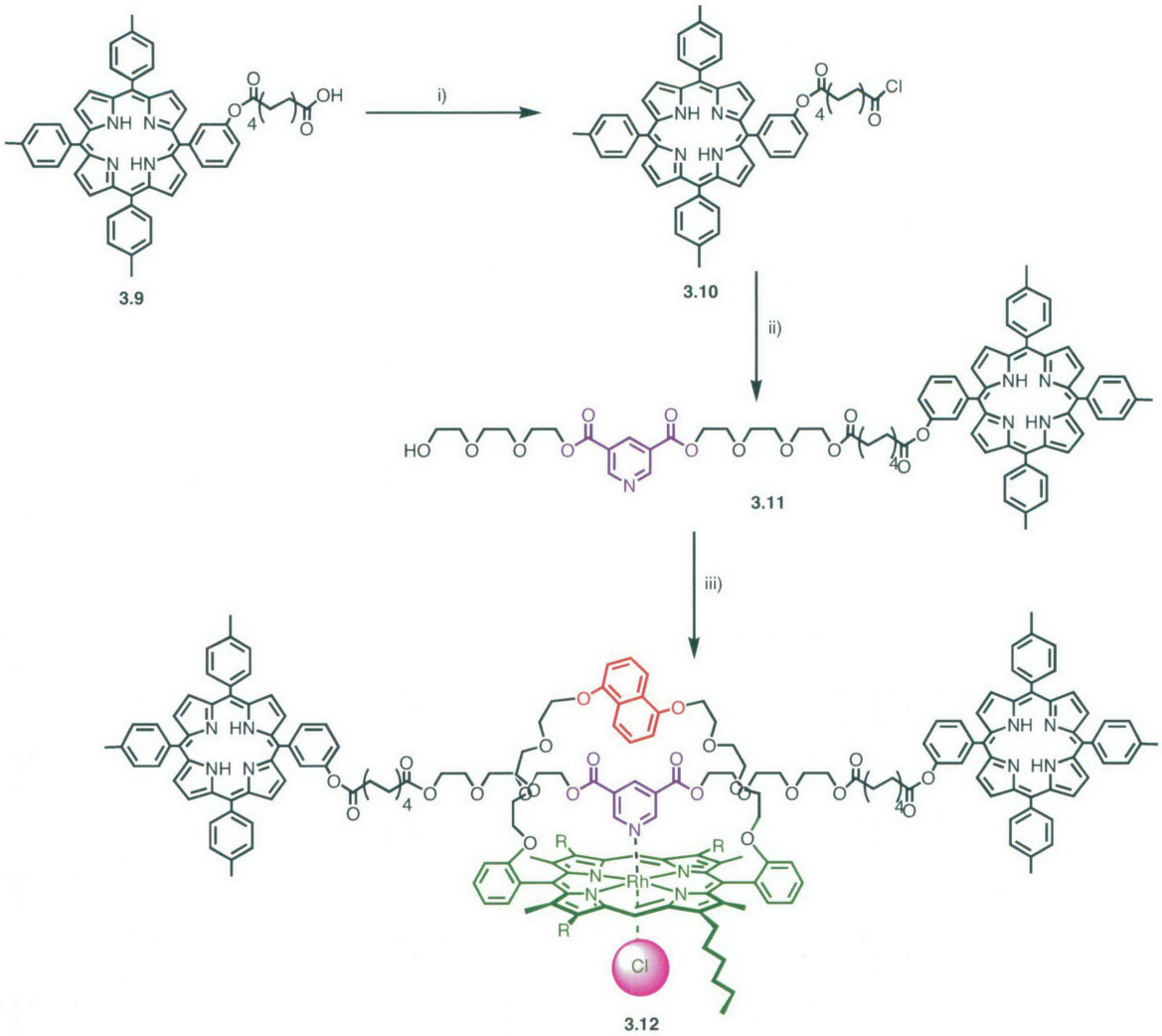

Scheme 3.4:- Reagents and conditions for the synthesis of rotaxane **3.12**; i) oxalyl chloride, 2 h RT, ii) **3.6**, dry $CHCl_3$, 16 h RT, iii) **3.5**, **3.10**, toluene, 16 h RT.

The acid chloride reaction was performed in the absence of any base such as triethylamine to preclude competition for the rhodium (the free base porphyrin itself can act as a base to neutralised the HCl formed in the reaction). Porphyrin **3.9** was stirred in excess thionyl chloride and dry toluene to produce the acid chloride porphyrin stopper **3.10**. This was reacted with the mono-porphyrin pyridine thread **3.11** in the presence of rhodium strapped porphyrin **3.5**; the expected product was the rotaxane **3.12**. Although the reaction between the thread and stopper proceeded as expected, nevertheless no rotaxane was obtained.

The ^{1}H NMR of the major rhodium porphyrin product showed clear resonances for bound pyridine protons at 6.23 and 1.83 ppm and the expected integration for a 1:1 rhodium

porphyrin macrocycle plus dumbbell complex. However split *meso* protons at 10.30 and 9.95 ppm, as well as split hexyl and methyl side chains were evident which is not expected in a rotaxane conformation. Furthermore only one set of peaks for the strapped porphyrin naphthalene aromatic protons (7.07, 6.31 and 5.48 ppm) were evident. These patterns in the strapped porphyrin protons is not consistent with a rotaxane structure, but rather with one in which central pyridine is coordinated on the same side of the porphyrin as the strap, but is not interlocked through the cavity, as seen in previous studies involving coordination of bulky ligands to these strapped porphyrins (See Chapter 2, Section 2.4).

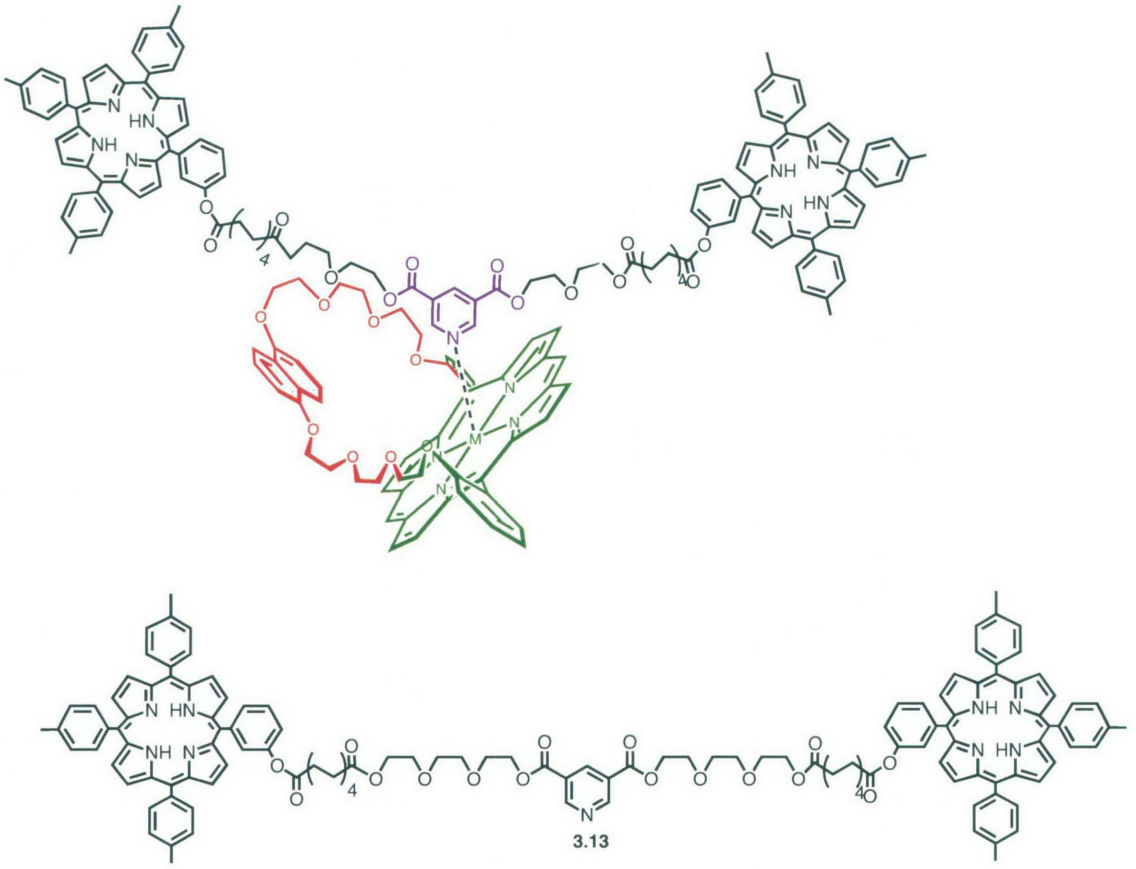

3.13

To confirm the proposed non-interlocked complex, repeated chromatography of this rhodium porphyrin mixture was performed. This revealed slow leaching of the dumbbell from the strapped porphyrin, as expected for a non-interlocked complex as the coordinated pyridine thread is eventually replaced by coordinating solvent (methanol). Indeed a 1:1 mixture of the rhodium porphyrin **3.5** and the mono-pyridine thread **3.11** also showed folding of the strap of the porphyrin to accommodate the pyridine ligand on the same side of the porphyrin as the strap, similar to that observed previously for bulky

pyridine ligands, as described in Chapter 2. This folding may be due to some π–π stacking interaction between the porphyrin stopper and the strapped porphyrin host. Nevertheless, although the concept of templating by the pyridine thread to the strap side of the Rh porphyrin was established, the flexibility of the strap allowed stoppering of the thread without it being linked through the aperture. Clearly new synthetic routes needed to be investigated.

3.5 "CLICK" CHEMISTRY-A NEW METHOD FOR ROTAXANE SYNTHESIS

The relatively new field of "click chemistry" that endeavours to expand the range of available reactions to produce heteroatom links between molecular modules, has grown rapidly. The key characteristics of "click chemistry" have been defined as reactions that allow diversity of subunits, give high yields, generate inoffensive by-products, use mild reaction conditions and have relatively straight forward workup and purification procedures.[8] Despite its popularity, the "click concept" has come under some criticism.[9] Nevertheless, one of the most productive reactions of this type that has found favour is the Cu(I) catalysed Huisgen 1,3-dipolar cycloaddition between alkynes and azides to give 1,2,3-triazoles (see Scheme 3.5). One notable advantage of this reaction is the relative ease by which both azide and alkyne functionality can be incorporated into a variety of different substrates and the comparative stability of the components once isolated. [8]

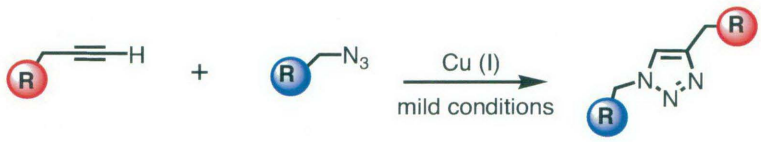

Scheme 3.5:- Cu (I)-catalysed Huisgen 1,3-dipolar cycloaddition ("click chemistry").

Numerous successful examples of this type of "click chemistry" have been reported using a wide variety of Cu(I) sources including various Cu(I) salts and complexes; in-situ reduction of Cu(II) salts by ascorbic acid which has been extensively used in aqueous systems; and (though less common) the oxidation of copper metal typically using nanosize Cu(0). [8, 10-13] The mild reaction conditions have led to this reaction gaining favour in the synthesis of supramolecular systems as the ability to perform these reactions

at room temperature or below, conditions which favour complexation, preorganisation or templating and result in higher yields of assembled species.

For example, Stoddart and co-workers have recently utilised this chemistry in the synthesis of both rotaxanes and a catenane incorporating cyclobis(paraquat-*p*-phenylene) macrocycles and naphthalene guests (see Figure 3.3).[11, 12] In both cases the Cu(I) source was from the reduction of $CuSO_4.5H_2O$ by ascorbic acid, both present in catalytic amounts. In their rotaxane attempts, yields of between 72-82% were obtained for various [2]-, [3]- and [4]-rotaxanes which was deemed far more efficient than corresponding clipping approaches which for the [4]-rotaxane was expected to result in only a 4% yield. Similarly, a direct comparison in catenane formation *via* copper-mediated Eglinton coupling and Huisgen 1,3–dipolar cycloaddition was performed, and it was found that the "click" type reaction gave nearly double the yield of catenane (41% compared to 21%).[12] The authors attributed the higher than expected rotaxane and catenane yields not only to the high yields typical of these click synthetic pathways, but also due to mild reaction temperatures (-10 °C for rotaxane and 23 °C for catenane synthesis) which favours complexation and results in a higher proportion of interlocked molecules than other reaction pathways which require heating.[11, 12]

Stoddart has also successfully used click reactions to stopper multistation rotaxanes incorporating the same macrocycle and a 1,5-dioxynaphthalene (DNP) unit, but also including a tetrathiafulvalene (TTF) unit.[14] It was shown that the triazole rings, introduced into the rotaxane during the click reaction, do not compete for recognition by the tetracationic cyclophane unit as it is switched between the TTF and the DNP unit during redox cycling.[14]

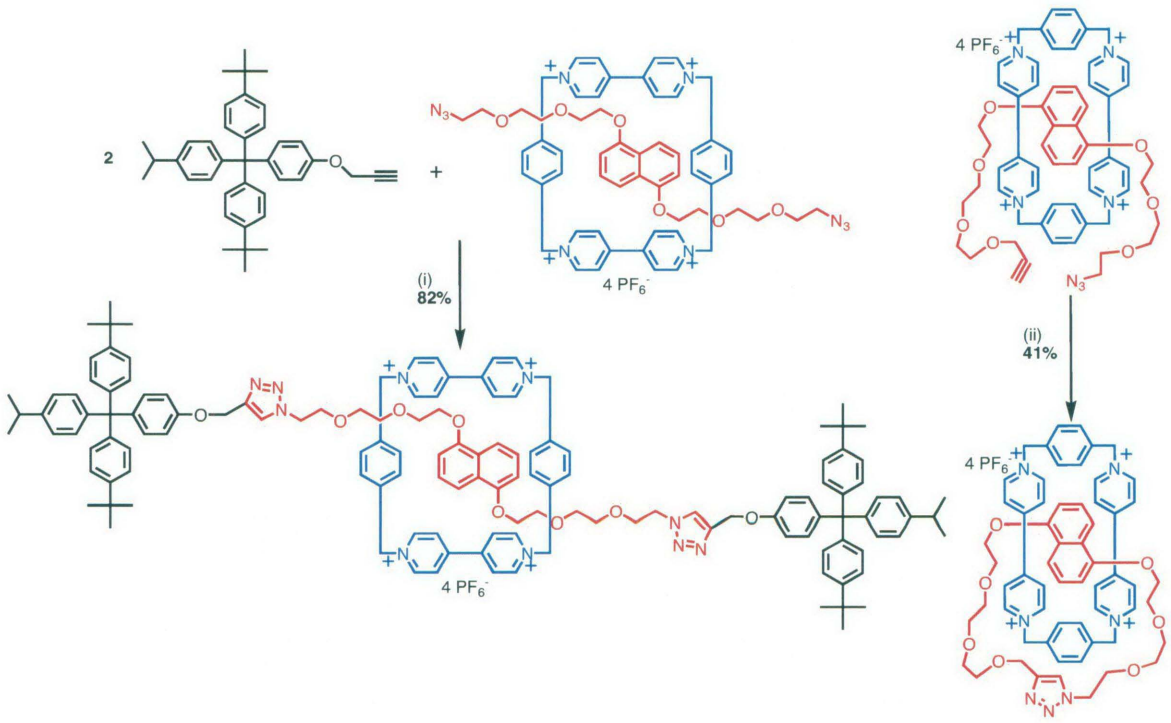

Figure 3.3 :- Stoddart's examples of using click chemistry to synthesis rotaxanes and catenanes.[11, 12] Reagents and conditions i) $CuSO_4.5H_2O$, ascorbic acid, DMF, -10 °C; ii) $CuSO_4.5H_2O$, ascorbic acid, DMF, 23 °C.

Specifically, for systems such as ours, it is preferential to use non-coordinating non-aqueous solvents, conditions which favour Cu(I) salts as the catalyst. Leigh *et. al.* have synthesised the rotaxane shown in Figure 3.4 using this click reaction with the organic–soluble Cu(I) salt $Cu(CH_3CN)_4PF_6$ as the catalyst.[10] It has been shown that in organic solvents the addition of bases such as DIPEA or 2,6-lutidine considerably enhances reaction rates[8, 10] and this needs to be considered in the synthetic planning. Leigh's systems however have an incorporated pyridine moiety in the macrocycle, negating the need for addition of an external base. This also acts as a template, as it provides a coordinating site for the Cu(I) ion. The rotaxane was formed in good yields (57%). They also investigated a variety of different reaction conditions, finding that overall conversion to triazole and rotaxane yields were dependent on variations in solvents, equivalents of copper catalyst, temperature and addition of other bases, specifically pyridine.[10]

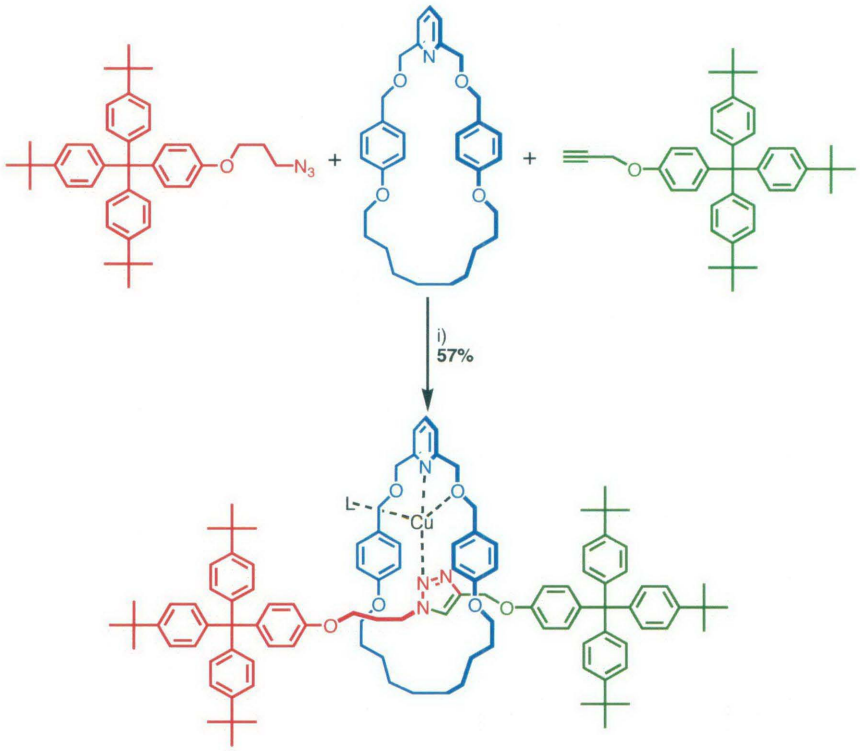

Figure 3.4:- Leigh *et al.* example of incorporating base into structure to enhance Cu I catalysis.[10] Reagents and conditions i) $Cu(CH_3CN)_4PF_6$, DCM, RT, 4 days.

Another advantage of using the click reaction to produce the 1,2,3 triazoles in our systems, is that the triazole could potentially coordinate to the metalloporphyrin. This provides the opportunity of an alternative binding site that could be introduced directly by the coupling procedure. So for example using a neutral diimide thread component, the triazole formed *via* the reaction can act as a second function or "station" in the final product; multi-station rotaxanes and catenanes can thus be easily accessible.[§] Thus, it was envisioned that the reaction of an azide functionalised diimide such as **3.17** with an alkyne blocker **3.14** in the presence of zinc strapped porphyrin **3.2** could yield a two station rotaxane in which the porphyrin was preferentially bound to the triazole. Shuttling to the diimide could be effected in protonating conditions (see Scheme 3.6). This reaction also may provide mild enough conditions to obtain a rhodium chloride rotaxane or catenane using pyridine templating, analogous to the concepts and procedures discussed above.

[§] Although this assumes, and we expect, that the 1,2,3-triazole moiety will act as a ligand to a variety of metalloporphyrins, nevertheless to the best of our knowledge no previous investigation into the binding of these types of triazoles to metalloporphyrins has been reported.

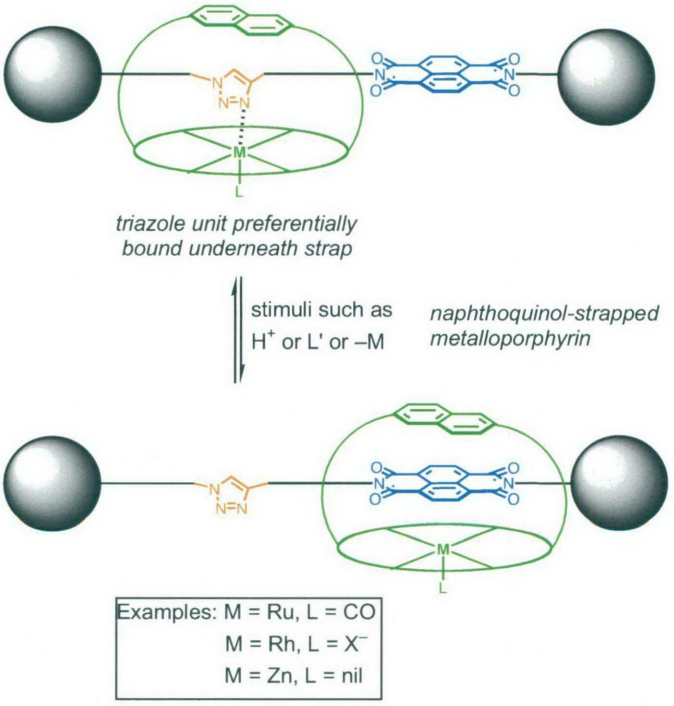

Scheme 3.6:- Schematic illustrating rotaxane dynamics utilizing triazole/metalloporphyrin coordination, and a neutral naphthodiimide unit. Protonation of the triazole, addition of exogenous competing ligand L' or removal of the metal ion are several of many factors that can be used to reversibly 'drive' the rotaxane.

Thus a variety of starting alkyne and azide components were synthesised to allow diversity in the design of rotaxanes *via* this click reaction (see Scheme 3.7). The crown **3.16**[15] and strapped porphyrin **3.2**[6] were synthesised according to literature procedures. The stopper **3.13**[16] was synthesised according to Stoddart's procedures, and the stopper alkyne **3.14** according to published procedures by Leigh[10]. The synthesis of diimide components **3.1**[7] and **3.19**[17] have also been previously reported.

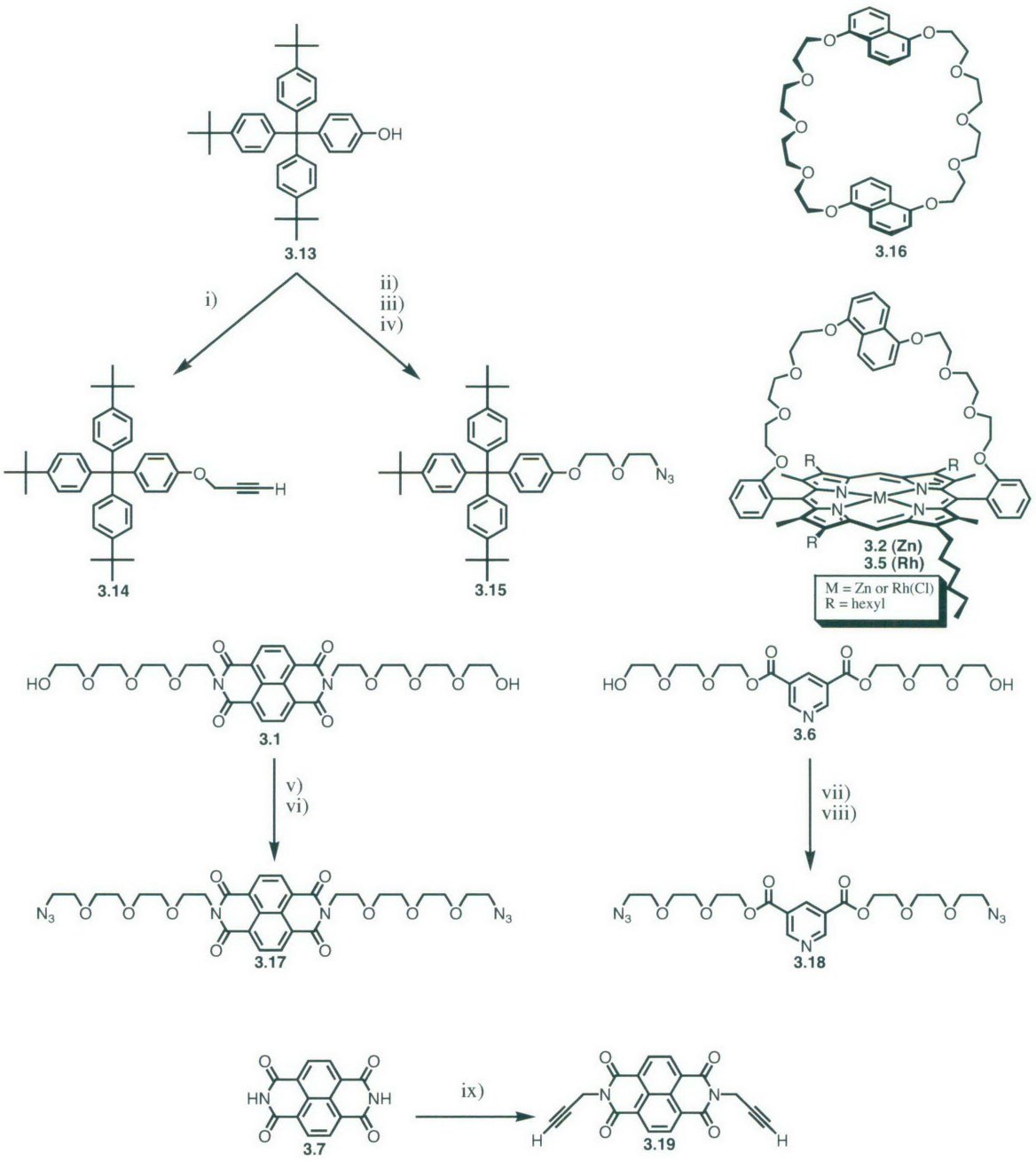

Scheme 3.7:- Reagents and conditions for the synthesis of a variety of alkyne and azide components for future rotaxane and catenane synthesis using "click" chemistry: (i) Propargyl bromide, K_2CO_3, DMF, 80 °C, 89%; (ii) 2-(chloroethoxyl)ethanol, K_2CO_3, MeCN, reflux 7 days, 70%; (iii) TsCl, DCM, 20%$NaOH_{(aq)}$, But_4NBr, RT 16 hours, quantitative; (iv) NaN_3, DMF, 60 °C, 16 hours, 63%; (v) TsCl, DCM, 20%$NaOH_{(aq)}$, But_4NBr, RT 16 hours, quantitative; (vi) NaN_3, DMF, 60 °C, 16 hours, 67%; (vii) TsCl, NEt_3, DCM, reflux, 7 days, 50%; (viii) NaN_3, DMF, RT, 4 days, 26%; ix) propargylamine, DMF, 140 °C, 4 hours, 59%.

Based on our premise that a diimide-triazole system could result in so-called "two station" threads with a metalloporphyrin shuttle as rotaxane components, control experiments were performed on the synthesis of dumbbell **3.20** from the diimide azide **3.17** and the stopper alkyne **3.14** to determine the ideal conditions for rotaxanes synthesis.

A variety of conditions was tested with the sources of Cu(I) ions arising from either the reduction of $CuSO_4.5H_2O$ by ascorbic acid or directly from the Cu(I) salt $Cu(MeCN)_4BF_4$, with and without added bases such as triethylamine and DIPEA (*N,N'*-diisopropylethylamine).

It was found that the best conditions were those using the Cu(I) salt $Cu(MeCN)_4BF_4$ (0.1 equivalent per alkyne) in dry degassed toluene and the addition of excess base (DIPEA, 2 equivalents). These conditions resulted in the formation of dumbbell **3.20** in 90 % yield.

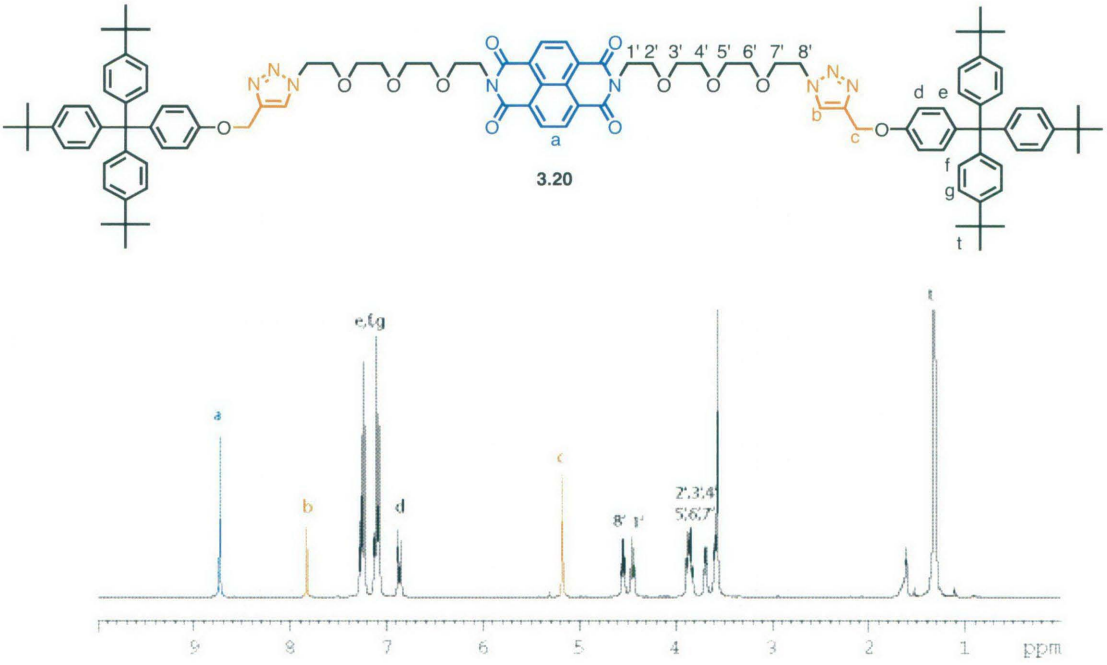

Figure 3.5:- ^{1}H NMR of dumbbell **3.20** (bottom); colours and non-systematic numbering of dumbbell **3.20** used in NMR assignment (top).

Characteristic ^{1}H NMR chemical shifts of the dumbbell were noted for comparison with such entities in the planned rotaxanes. It was found that the triazole protons b (Figure 3.5) had a chemical shift of 7.84 ppm and the methylene proton c shifted from 4.68 ppm in the alkyne starting material **3.14** to a singlet at 5.32 ppm in the dumbbell. The CH_2 proton 8' was substantially shifted downfield from 3.27 in the starting diimide azide **3.17** to 4.57 ppm. Small downfield shifts in the diimide and blocker protons (a and d) were also observed.

Having established the protocol for dumbbell formation using the click reaction, the reaction was attempted again in the presence of zinc strapped porphyrin **3.2** as a route to the rotaxane **3.21** (see Scheme 3.8).

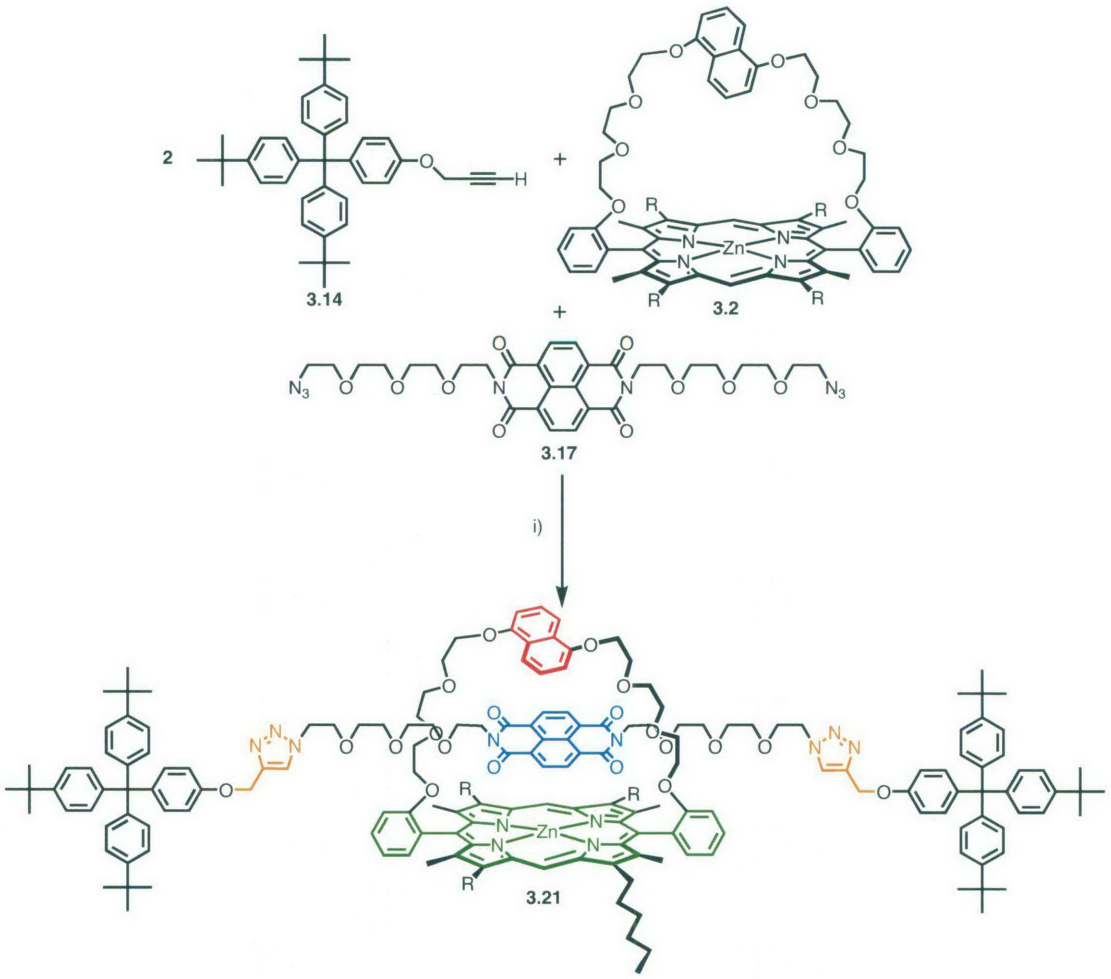

Scheme 3.8:- Reagents and conditions to produce rotaxane **3.21**; $Cu(MeCN)_4BF_4$, DIPEA, toluene, 4 days.

Unfortunately no rotaxane was isolated from the reaction mixture. The reaction between the azide and alkyne proceeded, however only dumbbell **3.20** and starting porphyrin material **3.2** were isolated. This could be explained by the fact that the binding of a structurally similar diimide precursor **3.1** was shown to be relatively weak (0.1 M^{-1}). Nevertheless despite this, catenanes incorporating the diimide moiety **3.19** have been made with these strapped porphyrins in up to 60% yields.[6] Thus the binding of the diimide precursors **3.19** used in these catenane studies warranted further investigation.

Initial attempts to carry out a standard binding constant measurement using an NMR titration of the guest **3.19** into a stock solution of strapped porphyrin **3.2** proved problematic due to the insolubility of the diimide in $CDCl_3$. Thus an alternative dilution procedure was performed. A stock solution of zinc porphyrin and solid, excess diimide was allowed to equilibrate, and over time, the diimide was solubilised by the porphyrin. Once the mixture had reached equilibrium (as judged by no further change in the NMR spectrum) the resulting solution was separated from excess solid and diluted sequentially to determine the binding constant (see Figure 3.6). It was found that the association constant K_a for this ligand was 799 M^{-1}, which was far higher than for the polyethylene glycol diimide derivative **3.1** which had been measured at 0.1 M^{-1}. It is likely that this is due to a combination of both the insolubility of the diimide** and the possibility of a C–H----O interaction between the relatively acidic hydrogens of the diimide alkyne and the oxygens in the strap of the porphyrin.[19] This could account for the fact that catenane reactions using ligand **3.19** were successful yet rotaxane attempts using diimide **3.17** were not.

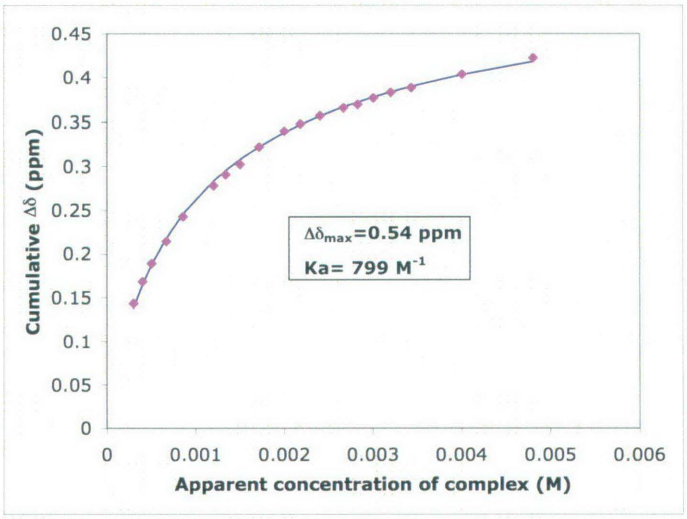

Figure 3.6:- Titration curve from the dilution NMR experiment of diimide **3.19** with strapped porphyrin **3.2**. The peak monitored throughout the titration was the diimide-CH_2.

** The overall binding constant of the complexation between a host and guest can be defined as: $\Delta G_{(complexation)} = \Delta G_{(Host\text{-}guest)} + \Delta G_{(solvent\text{-}solvent)} - \Delta G_{(host\text{-}solvent)} - \Delta G_{(guest\text{-}solvent)}$. In a binding equilibrium in which the guest has a low solubility the $\Delta G_{(guest\text{-}solvent)}$ becomes increasingly important. If solubility of the guest is high, this term will become more negative, resulting in a more positive $\Delta G_{(complexation)}$, ie weaker binding. If however the guest has low solubility in the chosen solvent, the $\Delta G_{(guest\text{-}solvent)}$ becomes only weakly negative or even positive resulting in a lower overall free energy, thus inducing a stronger than normal binding constant.[18]

Based on these results it was reasoned that the use of diimide alkyne **3.19** and blocker azide thread **3.15** to create an alternative rotaxane **3.24** might well be more successful. On the other hand under the conditions used in previous dumbbell formation the diimide **3.19** is not soluble, and this could hinder the reaction progress. Thus trial reactions were set up to establish the most viable reaction conditions. Two parallel reactions were carried out, one containing just the two components **3.19** and **3.15**, and the other with the addition of 1 equivalent of crown **3.16** which not only helps solubilise the diimide but also templates the reaction in favour of the rotaxane. All other conditions such as the amounts of $Cu(MeCN)_4BF_4$ and DIPEA and toluene were maintained the same in each case.

Due to the lack of solubility of the diimide, the system without added crown did not reach completion till 8 days, although it did successfully produce good yields of the dumbbell **3.22** (80%). However, in the reaction with 1 equivalent of crown **3.16**, not only was the reaction complete after 3 days due to the solubilisation of the diimide alkyne **3.19**, but the mild synthesis conditions resulted in the reaction producing the expected dumbbell **3.22** (46% yield) in addition to good yields of crown rotaxane **3.23** (43%) (see Scheme 3.9). The ESI-MS analysis of the crown rotaxane **3.23**, gave peaks *m/z* 2253.1 $[M+Na]^+$, 2237.1 $[M+Na]^+$, 2215.1 $[M+H]^+$, and 1129.8 $[M/2+Na]^+$, with very little fragmentation between M^+ and $M/2^+$ peaks, a feature characteristic of interlocked molecules (See Appendix 3, Figure A3.6).[20]

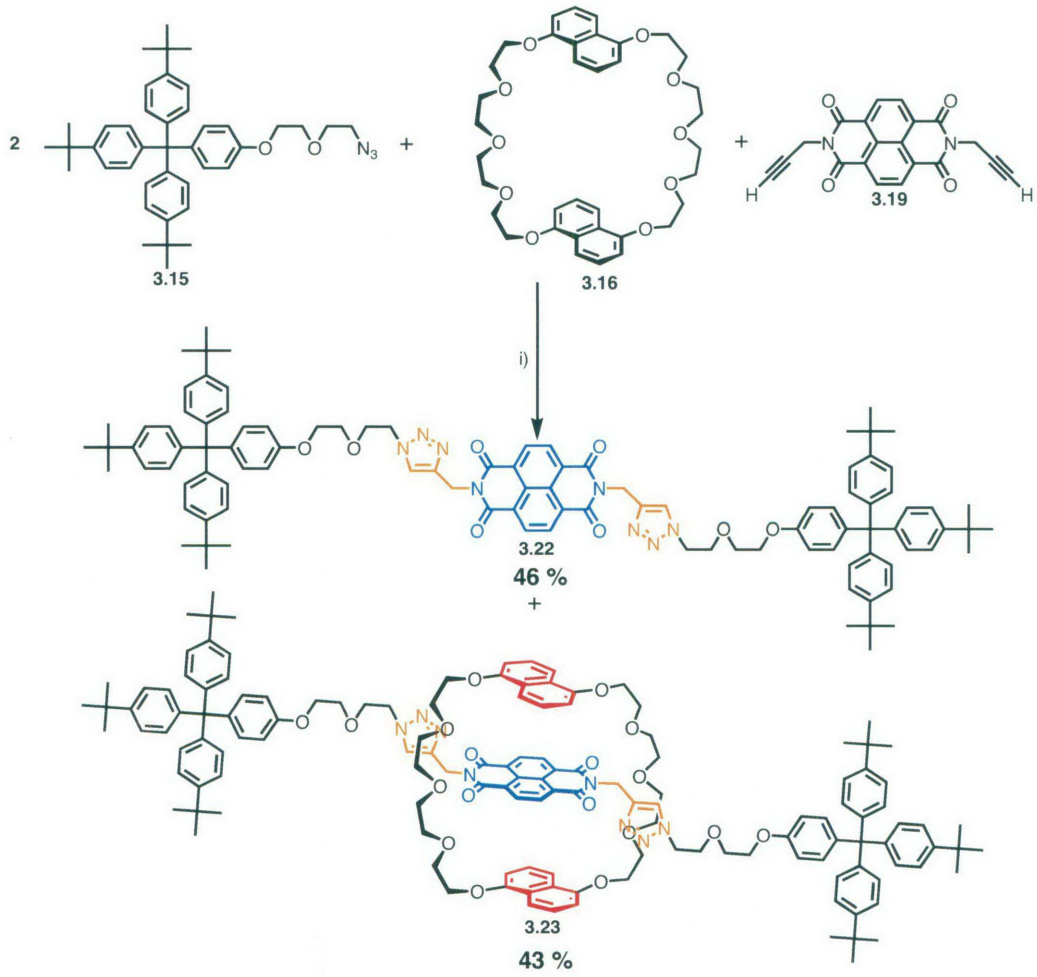

Scheme 3.9:- Reagents and conditions used to produce rotaxane **3.23** and dumbbell **3.22**; i) $Cu(MeCN)_4BF_4$, DIPEA, toluene, 3 days RT.

The structural confirmation of both the dumbbell **3.22** and the crown rotaxane **3.23** were obtained primarily using proton NMR, gradient COSY and NOESY techniques (See Figure A3.1 and A3.2 in Appendix 3). Figure 3.7 shows the non-systematic numbering system used to compare the dumbbell **3.22** with the rotaxane **3.23** in their corresponding ^{1}H NMR spectra.

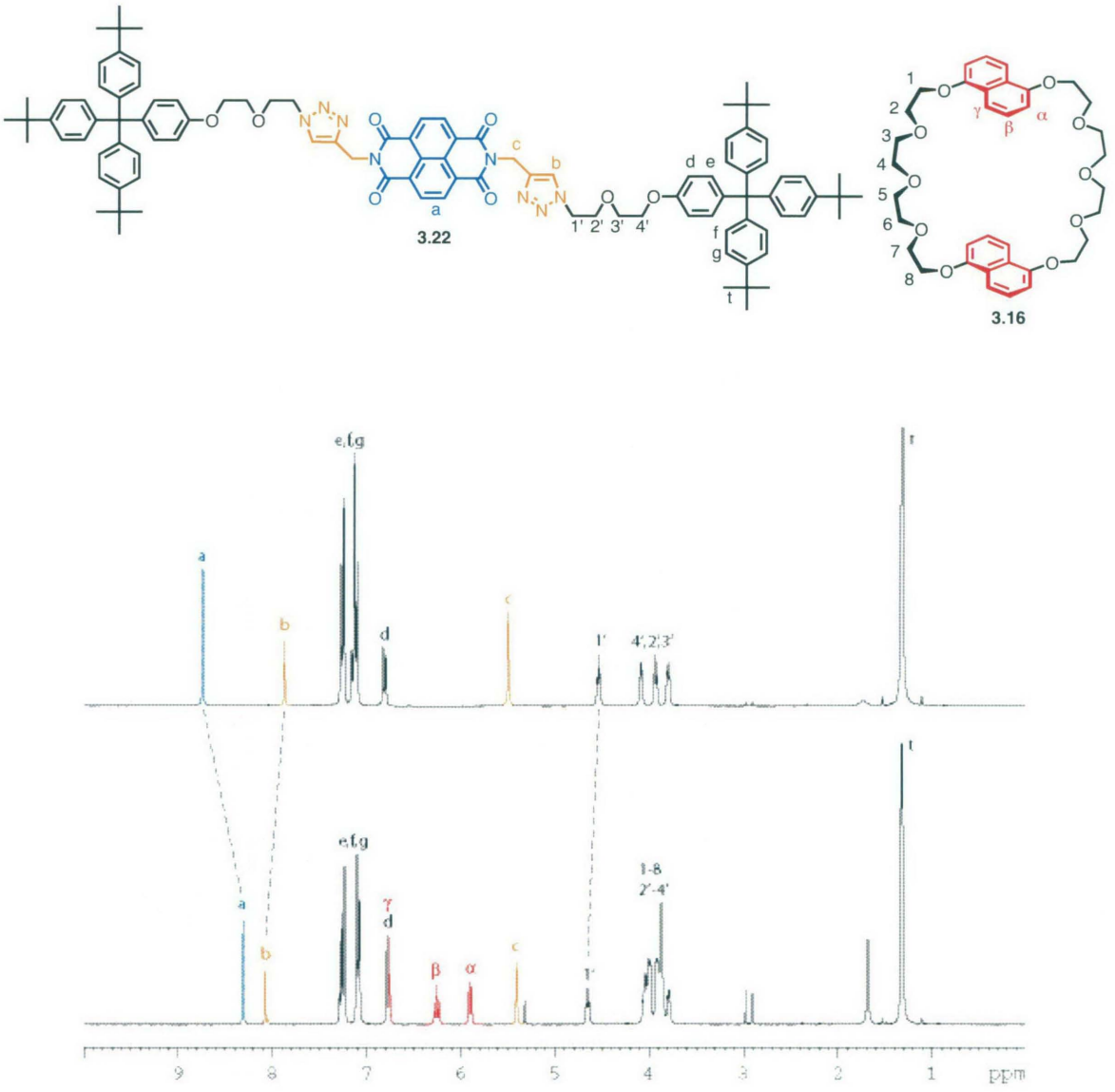

Figure 3.7:- ^{1}H NMR comparison of the dumbbell **3.22** (top) and the corresponding crown rotaxane **3.23** (bottom).

^{1}H NMR analysis of the dumbbell **3.22** showed the characteristic triazole peak b at 7.87 ppm and the OCH_2 proton c had shifted from 5.01 in the alkyne precursor **3.19** to 5.50 ppm in **3.22**. As with dumbbell **3.20**, the CH_2 proton 1' was also substantially shifted downfield from 3.43 ppm in the starting stopper azide **3.15** to 4.53 ppm in the dumbbell **3.22**. Small downfield shifts in the NDI and stopper peaks (a and d) were observed. All of these shifts are consistent with both the dumbbell **3.20** and those of similar published rotaxanes.[10, 11]

^{1}H NMR analysis of the crown rotaxane however revealed significant upfield shifts in both the naphthodiimide and crown protons. The diimide proton a is shifted upfield from 8.74 ppm in the dumbbell **3.22** to 8.31 ppm in the rotaxane **3.23** which is indicative of a shielding effect from the crown. The extent of this shift is comparable to other systems in which this crown is bound around a naphthodiimide thread.[15, 19, 21] Similarly, the crown peaks (α, β, γ) have been shifted upfield, appearing at 6.77, 6.26 and 5.90 ppm in the bound rotaxane as compared to their typically unbound positions of 7.79, 7.19 and 6.53 ppm. Again this is due to shielding by the diimide moiety indicative of binding of the crown to the guest in a co-facial arrangement. Triazole proton c, which is adjacent to the naphthodiimide, also had a slight upfield shift of 0.1 ppm. In similar diimide-crown catenanes, published by Sanders[19], the protons peripheral to the naphthodiimide moiety, showed shielding shifts of around 0.3 ppm and appeared as an AB system. The different splitting pattern and extent of shielding in our crown rotaxane structure is due to the greater conformational freedom associated with rotaxanes as compared to their typically more restricted catenane counterparts.

Conversely, the triazole peaks b and 1' were shifted slightly downfield from 7.87 to 8.08 ppm (b) and 4.53 to 4.65 ppm (1'). This is possibly due to the orientation of the 5 membered triazole ring being in the deshielding region of the crown aromatics, resulting in edge to edge interactions between triazole proton b and crown protons (α, β, γ).

NOESY experiments showed clear NOE's between the NDI proton a and the protons in the crown ethoxy units (see Appendix 3, Figure A3.1 and A3.2).[††] Weaker NOE's were also detected between the naphthodiimide protons and the most upfield crown aromatic proton (α) (this is often not seen in pseudorotaxane systems, however due to the permanent interlocking in the rotaxane close contacts are now more confined and thus detectable).

[††] The crown ethoxy proton peaks (1-8) overlap significantly in the ^{1}H NMR spectra, thus the exact protons resulting in the close contact NOE to the diimide proton a cannot be specified.

Further evidence of strong complexation in the mechanically interlocked system arose from a UV spectrum of the crown rotaxane. The crown rotaxane is pink yet the individual components, the dumbbell and the crown itself, are white/yellow. The colour arises from a charge transfer interaction between the crown and the diimide and appears at 500 nm with an extinction coefficient of 745 $M^{-1}cm^{-1}$ (see Figure 3.8). This has been observed in related crown-diimide catenane systems with charge transfer bands appearing between 480 and 530 nm with typical extinction coefficients of between 350-880 $M^{-1}cm^{-1}$.[22]

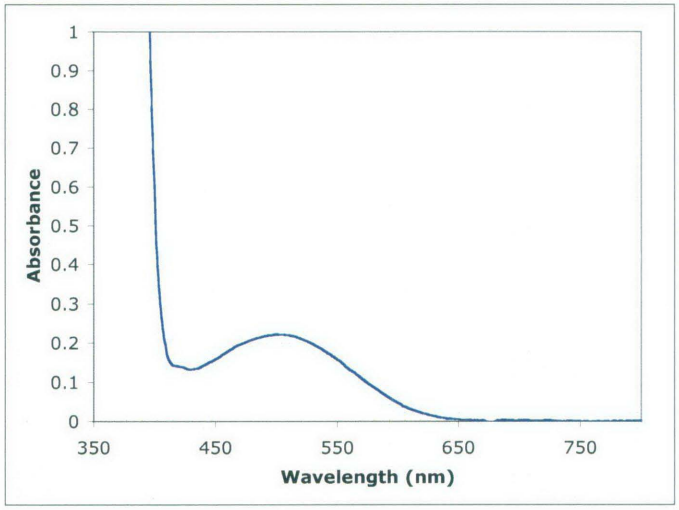

Figure 3.8:- Absorption spectra of the crown rotaxane **3.23** (concentration = 2.98×10^{-4} M^{-1}).

Having established that these components can be used to create both dumbbells and crown rotaxanes, the experiment was repeated again but in this case in the presence of the zinc strapped porphyrin **3.2** (see Scheme 3.10). It was envisioned that the stronger interaction between the strapped porphyrin and this diimide (compared to the diimide thread **3.17** in the previous route) would enable rotaxane formation.

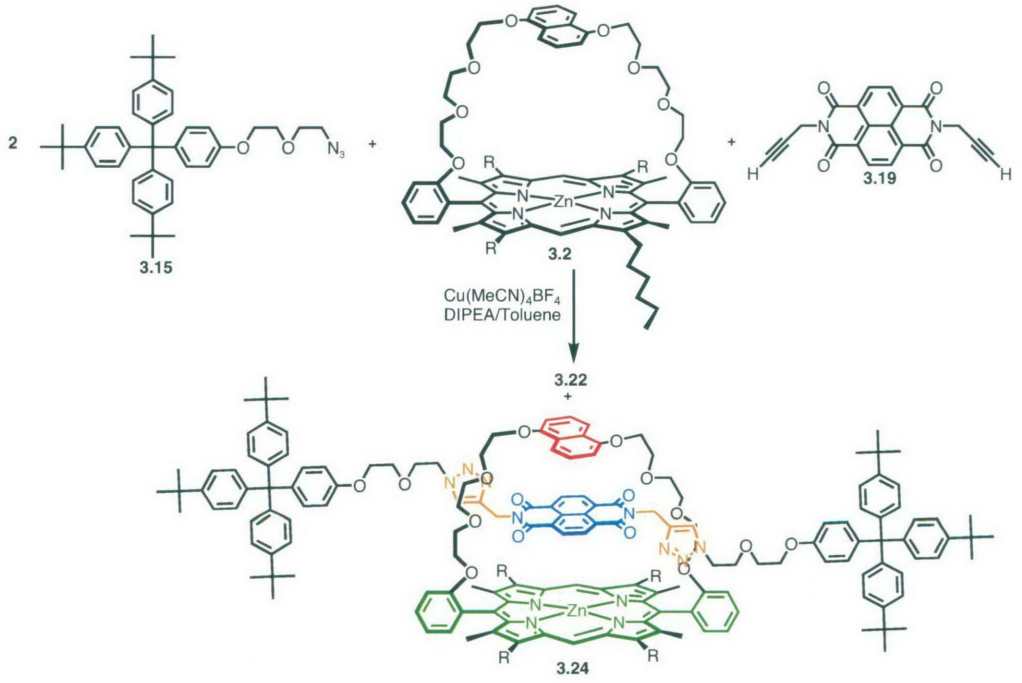

Scheme 3.10:- Reagents and conditions for the synthesis of porphyrin rotaxane **3.24**; $Cu(MeCN)_4BF_4$, DIPEA, toluene, 3 days RT.

After 3 days the reaction was complete, producing both dumbbell **3.22** (55%) and the porphyrin rotaxane **3.24** (20%). To date this is the first successful reaction producing a strapped porphyrin-diimide rotaxane in reasonable yields. This is undoubtedly due to the use of the stronger binding diimide **3.19** and the mild reaction conditions afforded by this type of "click" chemistry. Furthermore the strapped porphyrin starting material that was not entrapped during rotaxane synthesis was recovered intact (75%) indicating that the reaction is not destructive of this component. Although we made no attempts to optimise the yields of this reaction, presumably the yields of rotaxane can be enhanced by the use of (recoverable) excess strapped zinc porphyrin.

The ESI-MS analysis of the porphyrin rotaxane **3.24**, gave peaks *m/z* 2916 $[M+H]^+$, and 1459 $[M/2+H]^+$, with again very little fragmentation between M^+ and $M/2^+$ peaks, a feature characteristic of interlocked molecules (See Appendix 3, Figure A3.7).[20]

^1H, COSY and NOESY NMR studies were used to characterise the porphyrin rotaxane **3.24** (see Figure 3.9 and Figure A3.3 in Appendix 3). The most surprising aspect of the ^1H spectrum of **3.24** was the position of the diimide resonance a, which was significantly

upfield relative to its position in the uncomplexed dumbbell component, moving from 8.74 to 6.43 ppm. This is due to substantial shielding from the porphyrin ring consistent with a bound conformation. The triazole protons b however at 7.79 ppm were only shifted slightly upfield (0.08 ppm) indicating that the triazole is not coordinated to the zinc porphyrin as might be expected. This shows that any coordinate covalent binding of the triazole to the zinc is much weaker than the non-covalent binding of the diimide under the naphthoquinol strap of the porphyrin.

In the rotaxane the porphyrin proton resonances also displayed significant shifts from their respective positions in the strapped porphyrin with the most dramatic shifts observed for the naphthoquinol protons (γ, β, α) moving from 7.10, 6.39 and 5.38 ppm to 5.87, 5.23 and 4.66 ppm respectively. Shielding of the porphyrin *meso* protons was observed as indicated by an upfield shift of 0.36 ppm. These porphyrin and diimide shifts are consistent with a structure in which the diimide is located co-facially between the porphyrin and the naphthoquinol aromatic rings. The proton γ has the greatest upfield shift, indicating that it is in the most centrally located position above the aromatic ring of the diimide. In addition to this, the porphyrin methylene protons h4 are diasteriotopically split, which is to be expected in a structure in which the facial differentiation of the porphyrin is enhanced.

Conversely, the ethylene protons in the strap of the porphyrin are all shifted downfield by various degrees. The protons 18 and 19 exhibit the most deshielding (1.18 and 1.32 ppm respectively) and those above and below these positions to a lesser extent. This is due to the location of the porphyrin strap in the deshielding region (edge) of the diimide moiety, again confirming a co–facial arrangement of the diimide and porphyrin.

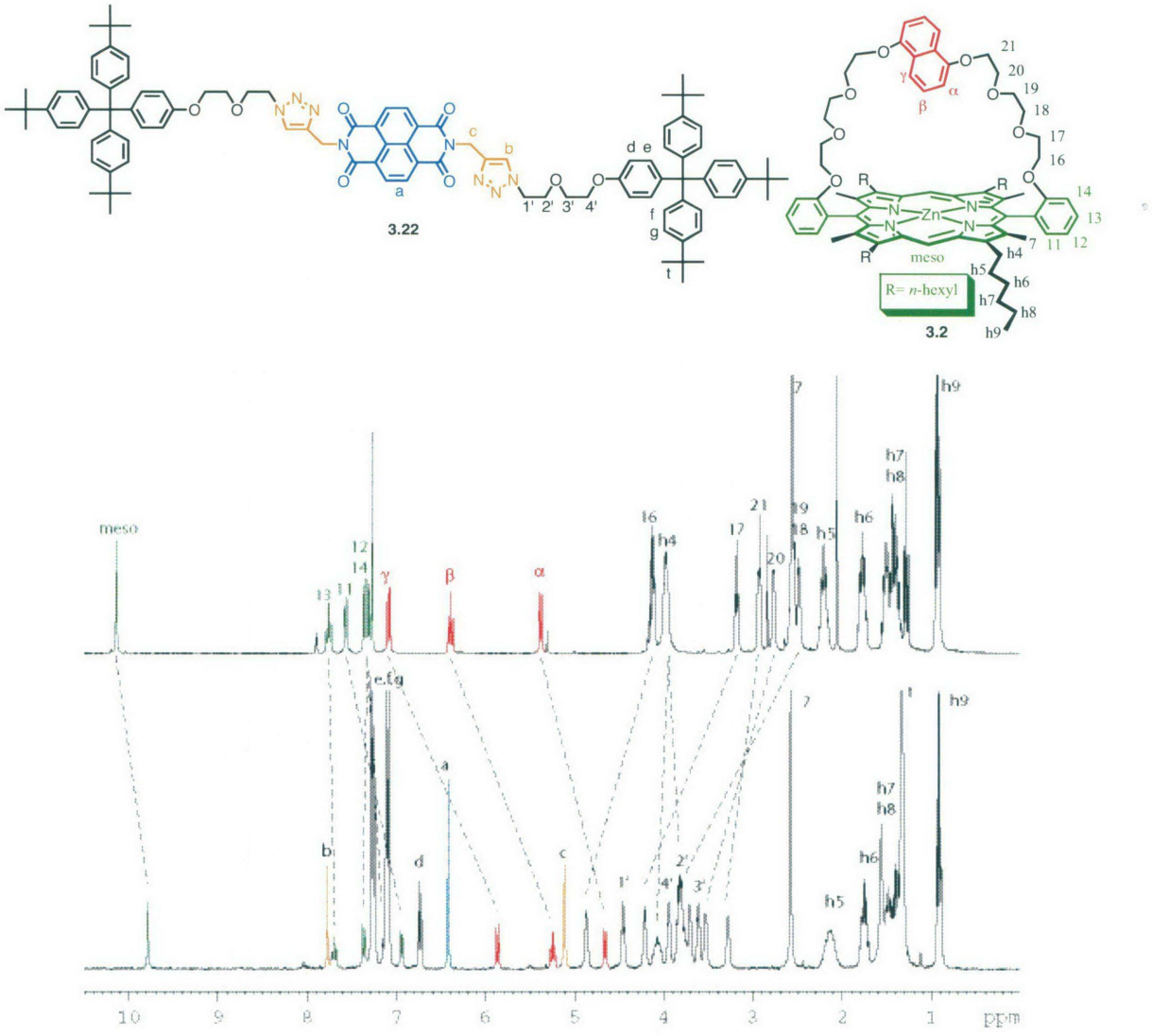

Figure 3.9:- ^{1}H NMR spectra of the strapped porphyrin **3.2** (top) compared to the porphyrin rotaxane **3.24** (bottom).

Variable temperature studies on this porphyrin rotaxane were performed to determine if at lower temperatures the complexation of the triazole to the zinc in the porphyrin might be favoured over diimide binding. As the temperature was decreased to –40 °C, no significant changes in the *meso* 1, diimide a or triazole b protons were observed, indicating that the diimide remains bound at lower temperatures, and is not displaced by competitive triazole coordination to the zinc.[‡‡]

[‡‡] Some upfield shifts in the a and b naphthoquinol protons and the ethoxy protons were observed as the temperature decreased which could be due to either conformational changes or possible weak intermolecular coordination of the triazole in the rotaxane to the zinc porphyrin of adjacent molecules, on the outside face, but this was not investigated further here.

Thus, despite having successfully synthesised a rotaxane containing a strapped porphyrin, which in itself is not insignificant, our goal of producing two–station rotaxanes directly by this route cannot be realised with this species as the triazole does not coordinate to the Zn ion in the metallated porphyrin. However, it was envisioned that if the zinc were replaced by a rhodium (III) ion in the strapped porphyrin then due to its higher affinity for nitrogen ligands, triazole coordination may be more favoured, allowing the possibility of "switching" to the diimide in protonating (or other) conditions.

In order to investigate the coordination behaviour of rhodium porphyrins towards the triazole entity, control experiments were first carried out, as we could find no literature reports on 1,2,3–triazole metalloporphyrin coordination. However, there has been one example of the potential of "click" triazoles to act as ligands in platinum and palladium transition metal complexes. In these cases it was found that their coordination strength is determined by their 1- and 4- substituents and typically, their coordination is about as strong as pyridine ligands.[23]

As a simple model for this the mono-triazole thread, **3.28** was synthesised from stopper alkyne **3.14** and stopper azide **3.15** *via* the standard click methodology previously discussed. ^{1}H NMR spectra of a mixture of this mono-triazole thread **3.28** plus one equivalent of iodo-rhodium (III) tetra tolyl porphyrin **3.25** are shown in Figure 3.10.

Analysis of the proton NMR spectrum of the uncomplexed mono-triazole thread **3.28** showed the characteristic triazole peak b at 7.81 ppm and the OCH_2 proton c at 5.13 ppm. As with previous dumbbells **3.20** and **3.22** the CH_2 proton 1' was also substantially shifted downfield from 3.43 ppm in the stopper azide starting material **3.15** to 4.58 ppm in **3.28**. These shifts are consistent with those of similar triazole components in previously reported non-porphyrinic rotaxanes.[10, 11]

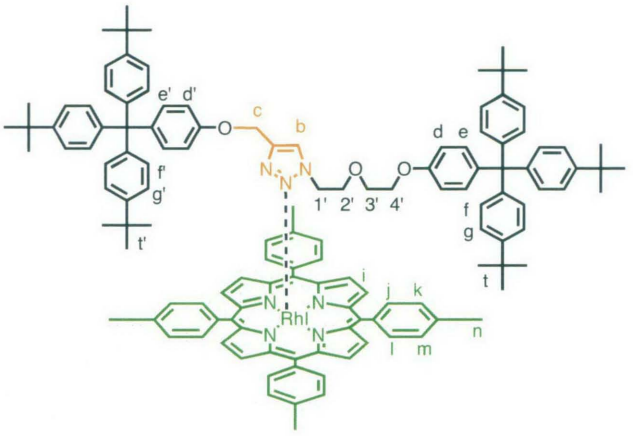

3.28

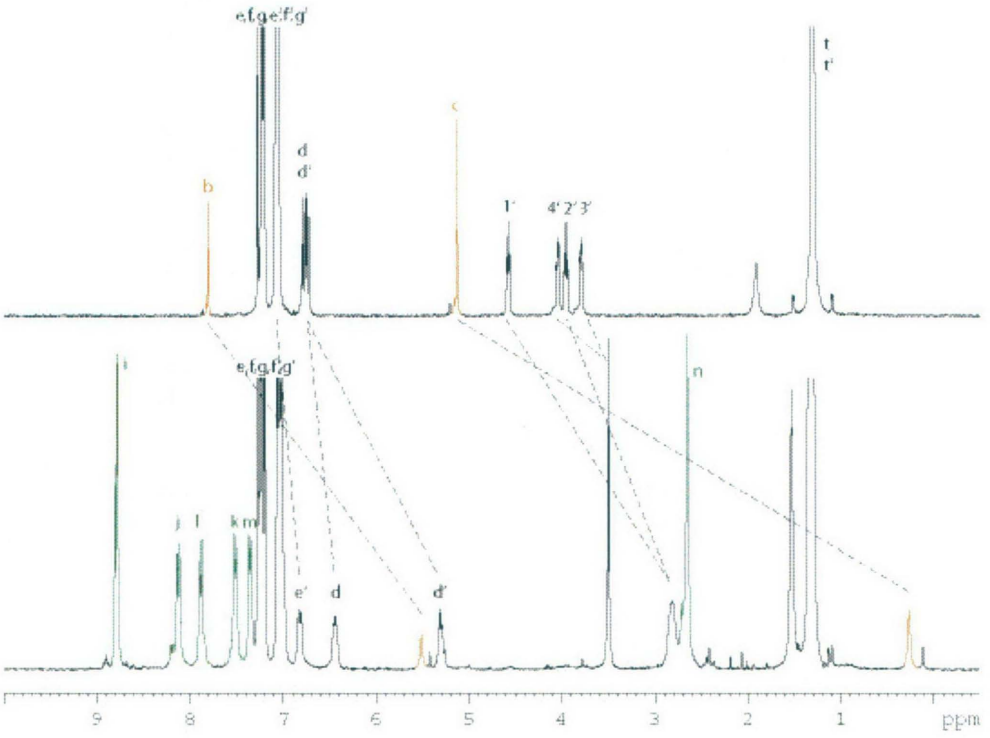

Figure 3.10:- ^{1}H NMR comparison of the mono-triazole thread **3.28** (top), and a mixture of thread **3.28** plus one equivalent of rhodium tetra tolyl porphyrin **3.25**.

Addition of one equivalent of rhodium porphyrin **3.25** resulted in significant upfield shifts in the triazole proton b from 7.81 to 5.51 ppm, with proton c shifting from 5.13 to 0.27 ppm, indicative of triazole coordination to the rhodium porphyrin. In addition to this, the stopper aromatics d and d' were also shifted upfield from 6.76 ppm in the mono-triazole thread **3.28** to 6.45 (proton d) and 5.32 ppm (proton d') due to shielding by the adjacent porphyrin. Interestingly the proton d' is significantly more shielded than proton d, due to the closer proximity of the porphyrin. Upfield shifts in the adjacent ethoxy protons (1'-4') were also observed, again as a result of porphyrin shielding.

Thus having established a model for the binding of triazole to rhodium porphyrins in a simple mono-triazole thread, attention turned to the more complicated *bis*-triazole dumbbell **3.22**. ^{1}H NMR spectra of a mixture of dumbbell **3.22** with two equivalents of iodo–rhodium (III) tetra tolyl porphyrin **3.25** (one equiv for each triazole) are shown in Figure 3.11.

At room temperature peaks for both the triazole and NCH_2-triazole protons b and c were not apparent in the ^{1}H NMR spectrum. In addition to this, the stopper aromatics d were shifted upfield from 6.82 to 6.49 ppm presumably due to shielding by the porphyrin. The ethoxy and the diimide protons (a, 1'- 4') were also shielded and upfield shifted.

At –20 °C the sharpened proton resonance for both the triazole and the OCH_2-triazole protons (b and c) appeared at 4.77 ppm and 0.42 ppm, respectively confirming the positions of the broadened and almost hidden resonances in the room temperature spectrum. Both peaks had significant upfield shifts, which is consistent with triazole coordination to the rhodium porphyrin. The upfield shift of the adjacent diimide and ethoxy protons are a result of porphyrin shielding.

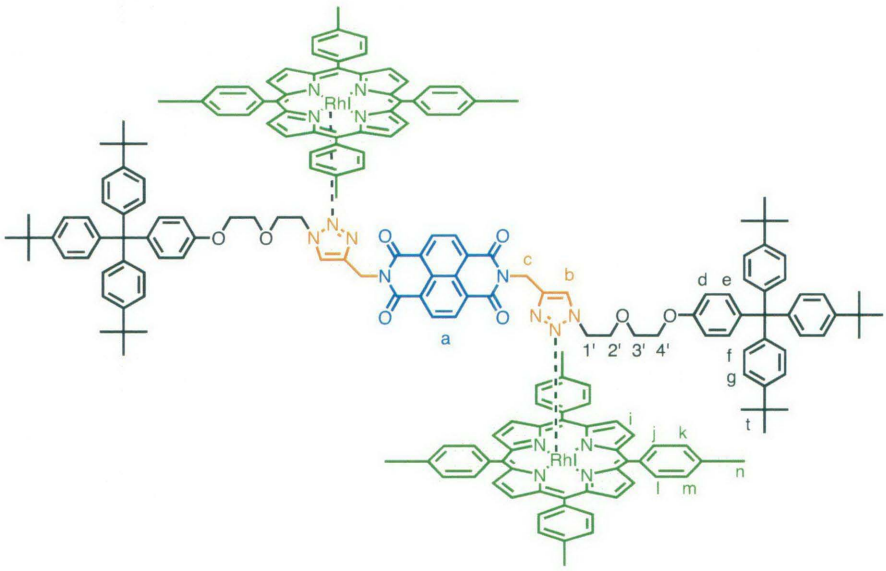

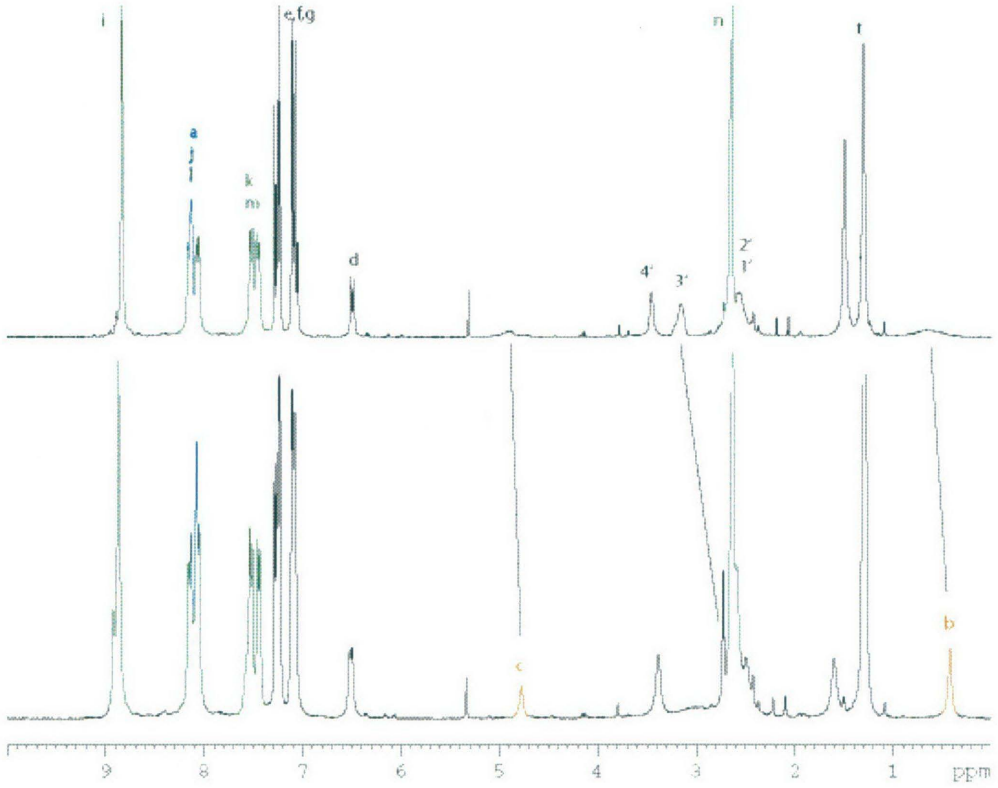

Figure 3.11:- ^{1}H NMR of a mixture of dumbbell **3.22** with 2 equivalents of rhodium porphyrin **3.25** at 30 °C (top) and –20 °C (bottom).

On first impressions, the fact that some protons in this system were broadened underneath the baseline (particularly protons b and c) at room temperature, suggests that the coordination of the triazole to the rhodium porphyrin might be in fast exchange on the NMR chemical shift timescale. However, closer inspection suggests that the system is not in "true" fast exchange by virtue of the NMR timescale. Although the peaks are broadened at 30 °C, their chemical shift does not change significantly with decreasing temperature as would be expected of a fast exchanging system. It is more likely that the triazole is fully coordinated, and the broadness at room temperature is caused by either undefined relaxation effects or exchange between the two coordinated porphyrins, rather than exchange between free and bound configurations. This is supported by the fact that the simple mono-triazole thread did not display the same broadness at 30 ° C, indicating that the coordination of triazole entities to rhodium porphyrins is not typically in fast exchange on the NMR chemical shift timescale.

Despite these control experiments with mono-triazole thread **3.28** and dumbbell **3.22** clearly showing triazole coordination to rhodium porphyrins, in the proposed rhodium

insertion into porphyrin rotaxane **3.24**, only one rhodium porphyrin for two possible coordinating triazole entities is present. A more realistic model, although considerably more complicated, is one in which only one equivalent of rhodium tetra tolyl porphyrin **3.25** is added to the *bis*-tiazole dumbbell **3.22**.

^{1}H NMR analysis of a mixture containing only one equivalent of rhodium porphyrin **3.25** with dumbbell **3.22** revealed that at 30 °C, many of the proton signals for the thread, diimide, and triazole protons were broadened under the baseline, presumably as a result of exchange between possible species in the mixture. At –20 °C however, the broadness had resolved and multiple peaks for each of the components were observed (see Figure 3.12). As expected the system was complicated, and three distinct coordination species were observed. A statistical mixture containing, uncoordinated dumbbell, mono-coordinated dumbbell, and di coordinated dumbbell was observed.

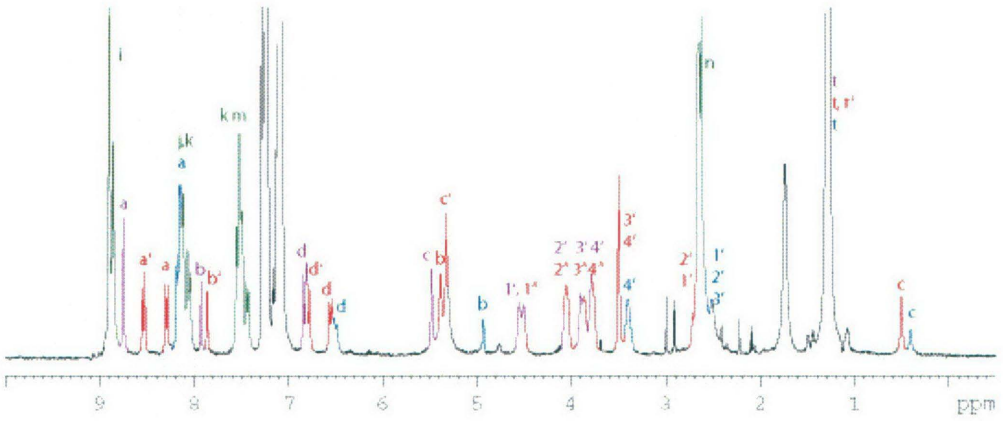

Figure 3.12:- ^{1}H NMR spectrum at -20 °C of a mixture of dumbbell **3.22** with one equivalent of rhodium porphyrin **3.25**. Purple colours indicate unbound dumbbell, blue colours indicate di-porphyrin coordinated dumbbell, and red colours indicate mono-coordinated dumbbell. For the mono-coordinated species two sets of peaks are evident with the coordinated side numbered as in Figure 3.11, and the uncoordinated side with additional ' ie. d', 1'' etc.

Of particular interest is the mono-coordinated species, as in a rhodium rotaxane no unbound or di-coordinated species can be obtained. The mono-coordinated species shows complete asymmetry, as expected due to the rhodium porphyrin binding only one of the two triazole entities present in the dumbbell. At –20 °C clear peaks for bound (5.40 ppm) and unbound (7.89 ppm) triazole proton b, and bound (0.53 ppm) and unbound (5.34 ppm) NCH_2 triazole proton c are evident. In addition to this, and because of the asymmetry, the diimide protons a are shifted upfield and split into two doublets at 8.52

and 8.31 (side closest to the porphyrin) ppm due to shielding by the porphyrin, as are the stopper aromatics at (6.78 and 6.54 ppm) and the ethoxy protons (1'- 4') in the thread. This asymmetric pattern can now be used as a model to decipher the ^{1}H NMR spectrum resulting from future rhodium insertion into rotaxane **3.24**.

Nevertheless, these control studies clearly show that the triazole moiety does indeed coordinate to rhodium porphyrins. Thus it was proposed that in the corresponding rhodium (III) derivative of porphyrin rotaxane **3.24**, switching between the triazole coordination and diimide complexation by the addition of acid or competing ligands may be possible, thus creating the first switchable rotaxanes incorporating these types of strapped porphyrin hosts.

Before rhodium could be inserted into the porphyrin rotaxane, the zinc needed to be removed, which is easily achieved by washing with dilute HCl. ^{1}H NMR analysis of the free base rotaxane **3.26** showed that the rotaxane remained intact. In this free–base derivative the diimide remained bound as evidenced by the upfield position of the diimide (6.36 ppm) and naphthoquinol resonances (5.88, 5.29 and 4.68 ppm). Indeed no significant changes in the NMR chemical shift patterns were observed compared to the zinc strapped porphyrin **3.24** except the presence of the porphyrin NH peaks that appeared at –4.27 ppm. These protons are significantly more upfield than typical free base porphyrins, which appear typically at around –2 to –3 ppm.[24] This is further evidence that the diimide is bound in the cavity of the strapped porphyrin in a co-facial arrangement and is shielding not only the naphthoquinol protons but also the porphyrin NH protons.

Having obtained the free base rotaxane **3.26**, the insertion of rhodium was attempted according to literature procedures (see Scheme 3.11).[25] Workup of the reaction afforded the rhodium iodide rotaxane **3.27** in 40% yield. It appeared that some of the rotaxane material was destroyed during the rhodium insertion, but nevertheless reasonable quantities of rhodium rotaxane were obtained.

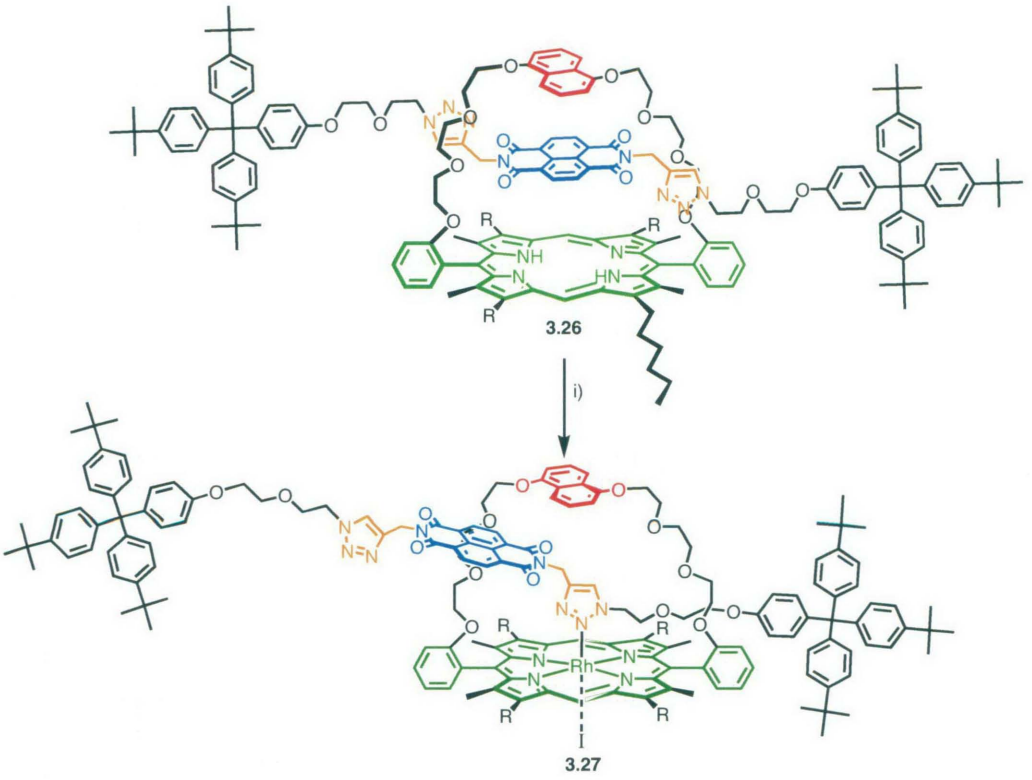

Scheme 3.11:- Reagents and conditions for the synthesis of rhodium iodide rotaxane **3.27**; i) $[Rh(CO)_2Cl]_2$, anhydrous sodium acetate, I_2, dry $CHCl_3$, 16 hours RT.

The ESI-MS analysis of the rhodium porphyrin rotaxane **3.27**, had a major *m/z* peak at 3082 representing the $[M+H]^+$ species with the iodide ligand remaining coordinated to the rhodium metal. Minor peaks at 2954 for the $[M-I]^+$ and 2986 for the $[(M-I)+Na]^+$ were also present (See Appendix 3, Figure A3.8).

Structural conformation of the rhodium rotaxane **3.27** was achieved primarily by ^1H, COSY and NOESY NMR (see Figure 3.13 and Figure A3.4 and A3.5 in appendix 3). At room temperature the peaks observed in the ^1H NMR spectrum were broad, indicative of fast exchanging processes. At –20 °C the spectrum had resolved considerably however, and two sets of peaks for many of the porphyrin and thread protons were apparent.

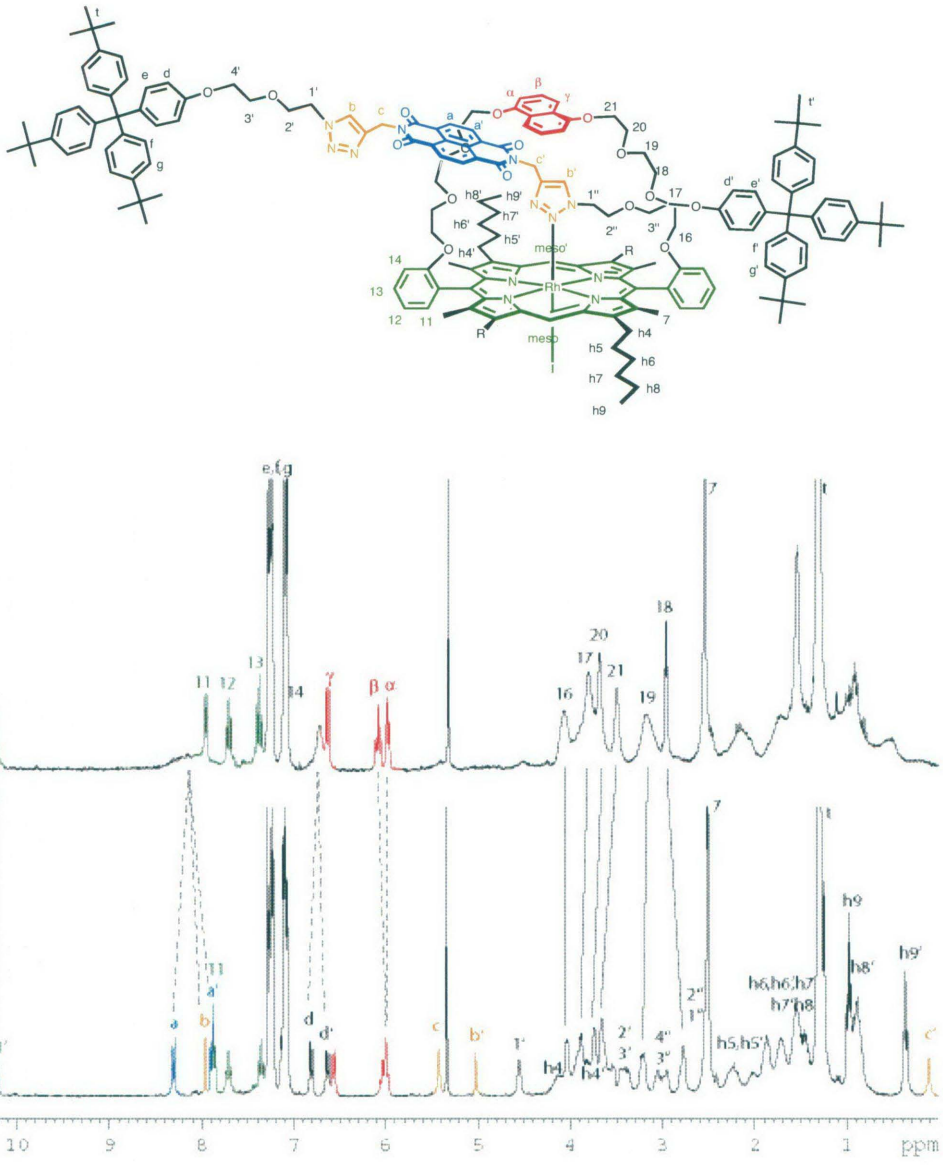

Figure 3.13:- Variable temperature ^{1}H NMR spectra of the rhodium rotaxane **3.27** at 30 °C (top) and –20 °C (bottom).

This asymmetry is due to the rhodium porphyrin binding only one of the two triazole entities present in the dumbbell and is similar to that seen in the mono-tetra tolyl rhodium coordination to dumbbell **3.22** discussed above. At –20 °C clear peaks for bound (5.02 ppm) and unbound (7.97 ppm) triazole proton b and bound (0.11 ppm) and unbound (5.43 ppm) NCH_2-triazole protons c are evident. The 1:1 proportion confirms that the porphyrin is coordinated to only one side of the thread and that the broadness at higher temperatures is probably due to a shuttling process between the two triazoles. Furthermore the diimide proton a is split into two doublets at 8.31 and 7.88 ppm, as are the stopper aromatics d at

6.62 (side close to the porphyrin) and 6.82 ppm (end furthest from porphyrin) as a result of the induced asymmetry.

The induced C_2 symmetry is also reflected in spilt porphyrin resonances. Thus the porphyrin meso protons and the methyl and hexyl protons are split into two peaks at –20 °C. However no asymmetry in the side aromatics of the porphyrin or the naphthoquinol aromatics in the porphyrin strap is observed indicating that these are reflected in the perpendicular mirror plane. NOESY experiments clearly show close contacts between the naphthoquinol and the bound triazole peak that confirms coordination of the triazole, and that the diimide moiety is thus displaced from the cavity (see Appendix 3, Figures A3.4 and A3.5).

Having fully characterised the rhodium rotaxane, and established that the preferred conformation is with coordinated triazole rather than bound diimide, investigations into the creation of a switchable rotaxane were initiated. A set of conditions under which the triazole coordination can be interrupted to allow the diimide to bind inside the cavity needs to be found in order to create controlled translational movement. Furthermore, this process needs to be reversible in order to create a "switchable" system.

One common method of inhibiting the binding of a ligand to metal ions is to use a competitively coordinating solvent. Thus 10% MeOD was added to the rhodium rotaxane **3.27** in $CDCl_3$ to determine whether firstly, the coordination of the triazole to the rhodium were inhibited, and secondly, if coordination were prevented, whether this would enable non-covalent binding of the diimide under the strap of the porphyrin. However on addition of the methanol no significant change in the porphyrin rotaxane was observed with the triazole remaining fully coordinated. Likewise deuterated acetone, (used as a solvent) did not compete with the triazole for coordination to the rhodium. The stronger ligand acetonitrile could not be used because of the insolubility of the rhodium rotaxane **3.27**.

As solvent did not appear to be able to create the right conditions for switching this rotaxane, attention turned to the use of acid to protonate the triazole and hence prevent its coordination to the metal. Control experiments were performed on a mixture of mono-triazole thread **3.28** coordinated to rhodium porphyrin **3.25** to establish the conditions needed to prevent triazole coordination. TFA in $CDCl_3$ was added to this mixture and NMR analysis performed (see Figure **3.14**).

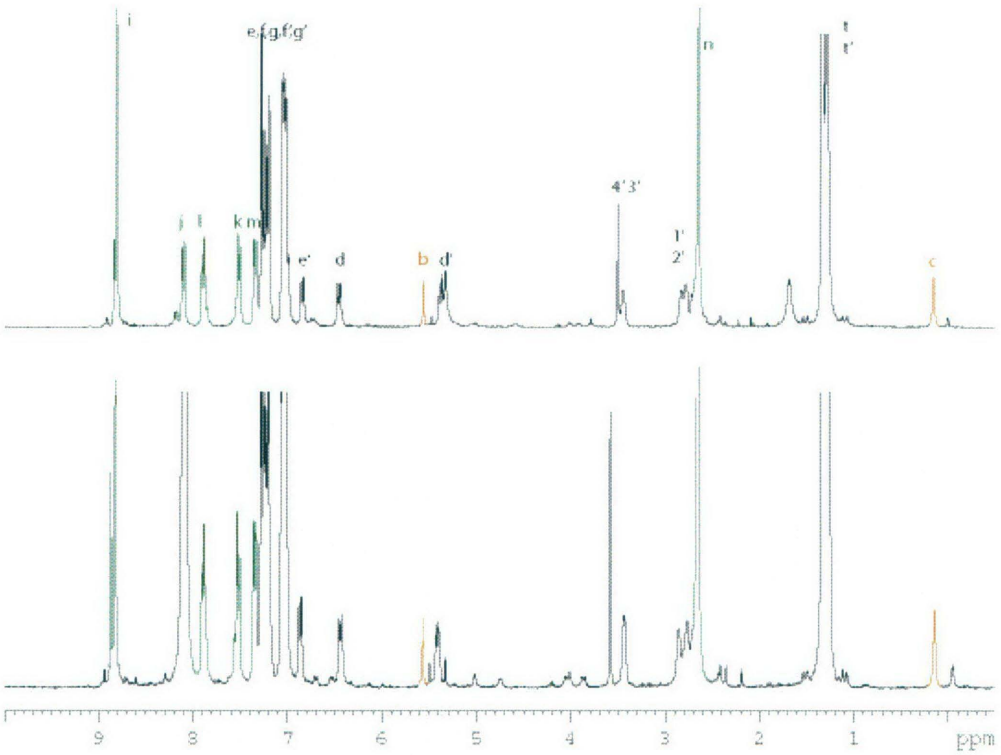

Figure 3.14:- ^{1}H NMR spectra at –20 °C of a mixture of rhodium porphyrin **3.25** and mono-triazole thread **3.28** (top), and the same mixture with 10 equivalents of TFA added (bottom).

At room temperature significant broadening of the triazole peaks b and c were observed upon addition of 10 equivalents of TFA. This might have at first indicated that the TFA was able to protonate the triazole and thus prevent its coordination to the rhodium porphyrin, however at –20 °C the ^{1}H NMR spectrum suggested otherwise. It appeared that the triazole was still coordinated as evident by the characteristic position of the triazole proton b at 5.58 ppm and the proton c at 0.15 ppm. The spectrum obtained was almost identical to that with no added TFA at –20 °C, indicating that the triazole remained coordinated to the rhodium despite the addition of acid. Even addition of 30 equivalents

of TFA[§§], did not prevent coordination of the triazole, however small peaks in the NMR spectrum did begin to arise, but whether these are due to uncoordinated thread or due to possible ligand swapping between the iodo ligand of the rhodium porphyrin **3.25** with trifluoroacetate is not definitive and was not investigated further. What is clear is that even in the presence of 30 equivalents of TFA, triazole coordination is not prevented, thus protonating conditions for rotaxane **3.27** would not induce an environment that would prevent coordination of the triazole and allow diimide binding. Again, alternative conditions needed to be investigated.

As competing solvents and protonation had proved to be inappropriate conditions in which the triazole coordination to the rhodium porphyrin in rotaxane **3.27** could be prevented, allowing diimide binding to occur, attention was turned to the use of stronger ligands, such as pyridine based ligands, to create a "switchable" rotaxane. Control studies were thus performed to find suitable ligands. Thus to a mixture of dumbbell **3.22** and 2 equivalents of rhodium iodide tetra tolyl porphyrin **3.25**, was added the di-substituted pyridine ligand **3.29** and ^{1}H NMR spectra were recorded (see Figure 3.15).

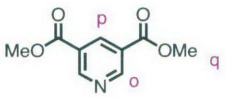

3.29

Addition of the pyridine ligand resulted in the immediate decomplexation and rupture of the triazole-rhodium bond as evidenced by the triazole protons b and c appearing at their typically unbound positions of 7.87 and 5.50 ppm respectively. Indeed all of the dumbbell proton peaks appeared in positions identical to that of the dumbbell starting material with no added porphyrin. Furthermore the protons associated with the pyridine ligand **3.29** appeared at 7.15 and 1.86 ppm, which is characteristic for coordination of this ligand to rhodium porphyrins as discussed in Chapter 2. This strongly suggested that the addition of pyridine based ligands to the rhodium rotaxane **3.27** may be able to prevent the triazole coordination to the rhodium *via* competitive binding. Thus one equivalent of pyridine

[§§] Addition of greater that 30 equivalents, was deemed impractical as any changes in the ^{1}H NMR is likely to be due to ligand swapping, or destruction of either the porphyrin or the thread. Harsh conditions could destroy future rotaxanes which is not conducive to reversible and controlled "switching", the aim of this project.

ligand **3.29** was added to a solution of the rhodium rotaxane and the NMR recorded (see Figure 3.15).

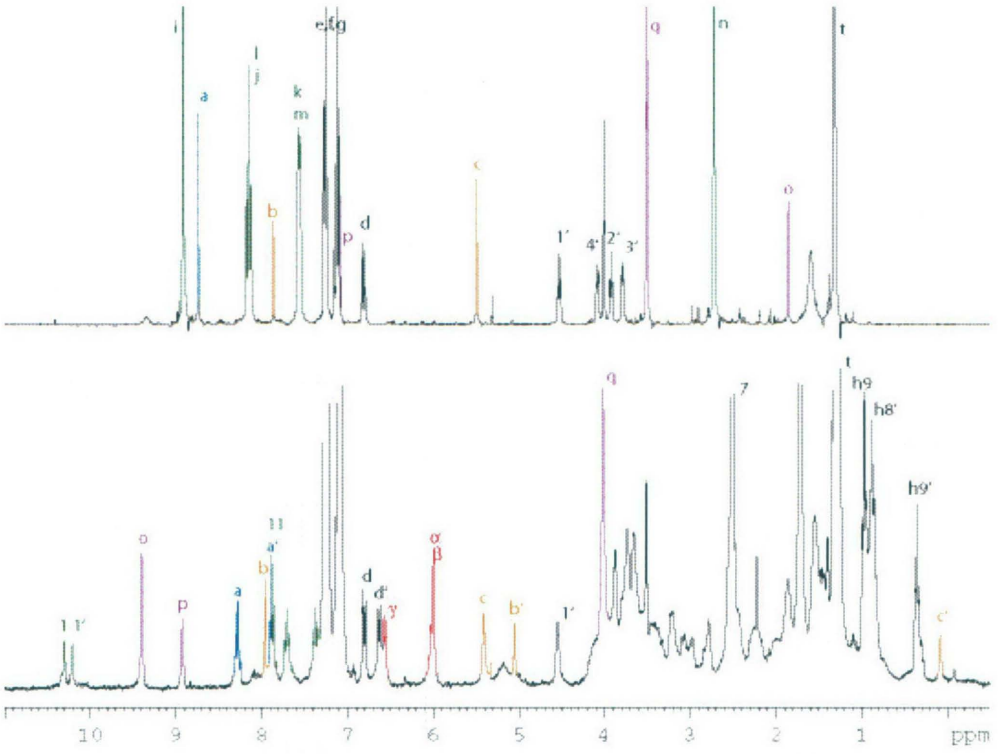

Figure 3.15:- ^{1}H NMR spectra of a mixture of dumbbell **3.22** + 2 equiv. rhodium porphyrin **3.25** + pyridine **3.29** (top); and a mixture of rhodium rotaxane **3.27** plus pyridine ligand **3.29** (bottom).

However, upon addition of the pyridine ligand, no evidence for the disruption of the binding of the triazole to the rhodium porphyrin was observed. In fact the protons associated with the pyridine ligand o and p appeared at their unbound positions of 9.39 and 8.91 ppm respectively, which confirms that they are not successfully competing with the triazole entity for coordination to the rhodium porphyrin. Variable temperature studies were performed to determine if at low temperatures the pyridine ligand can compete for binding, however no change was observed. It is clear that despite the control experiments indicating that this ligand would successfully compete for coordination, in simple Rh(III) porphyrins, the intramolecular binding mode of the triazole to the rhodium porphyrin in the rotaxane strengthens this interaction, preventing any effective competition.

As discussed in Chapter 2, the chosen pyridine ligand **3.29** is a much weaker ligand than pyridine itself, and thus it was envisioned that use of pyridine itself may provide the

added ligand strength needed to disrupt the strong intramolecular triazole-rhodium interaction. One equivalent of pyridine was added to the rhodium rotaxane **3.27** and ^{1}H NMR spectra were recorded. The proton spectra showed a new doublet appearing at 0.34 ppm which displayed characteristic pyridine COSY patterns coupling to protons at 3.76 and 4.40 ppm. This strongly suggested that the pyridine had successfully bound to the rhodium porphyrin; however variable temperature studies showed that as the temperature decreased, the pyridine proton shifted upfield. This is not characteristic behaviour of pyridine binding to the rhodium porphyrin, which is typically in slow exchange, and therefore temperature changes typically result in changes in peak intensity and not shifts in the peak position. In addition to this no typical unbound triazole peaks were evident in the ^{1}H NMR spectrum indicating either that they were still coordinated to the rhodium porphyrin, or that they were not coordinated but still under the strap of the porphyrin. Similarly, no characteristic bound diimide peak was observed as might be expected if the pyridine was coordinated to the outside face of the porphyrin, allowing diimide to bind in the cavity of the strapped porphyrin.

The system was very complicated, and it was thought that as in Chapter 2, it may resolve over time as exchange of the pyridine ligand from "inside" to "outside" coordination may occur. Unfortunately, over time it appeared that the rotaxane was decomposing. TLC analysis showed that the rotaxane had degraded into multiple porphyrin and non-porphyrin entities. This behaviour was not expected, and previous binding studies of rhodium porphyrin-pyridine complexes showed no such decomposition. It is thought that either electron transfer or redox reaction between the rhodium porphyrin and the diimide moiety may be occurring in the presence of oxygen, possibly resulting in free radicals which are capable of destroying the rotaxane. This rendered a full investigation into the binding of the pyridine too difficult as without the system reaching a stable equilibrium, a detailed analysis is prevented. It also suggests that the use of the rhodium porphyrin, despite showing promise, may not produce a rotaxane with these components that is capable of controlled, "reversible" switching, due to its instability.

3.6 THE USE OF PYRIDINE TEMPLATING IN THE SYNTHESIS OF ROTAXANES AND CATENANES *VIA* CLICK METHODOLOGIES

Despite successfully synthesising a rotaxane incorporating the strapped porphyrin as the macrocycle in reasonable yields, our original goal was to use metal ion-pyridine templating to not only template the formation of interlocked species, but also to potentially create a "switchable" rotaxane or catenane. Having established "click" methodologies as ideal in rotaxane formation due to their high yields and mild reaction conditions, trials were undertaken using similar conditions, but using the pyridine azide **3.18** as the template.

Initial studies into the viability of this reaction to produce rotaxane were undertaken, and reaction between the pyridine thread **3.18** and the stopper alkyne **3.14** to produce dumbbell **3.30** were attempted using the conditions established for the successful synthesis of previous dumbbells and rotaxanes **3.20**, **3.22**, **3.23**, and **3.24** (see Scheme 3.12).

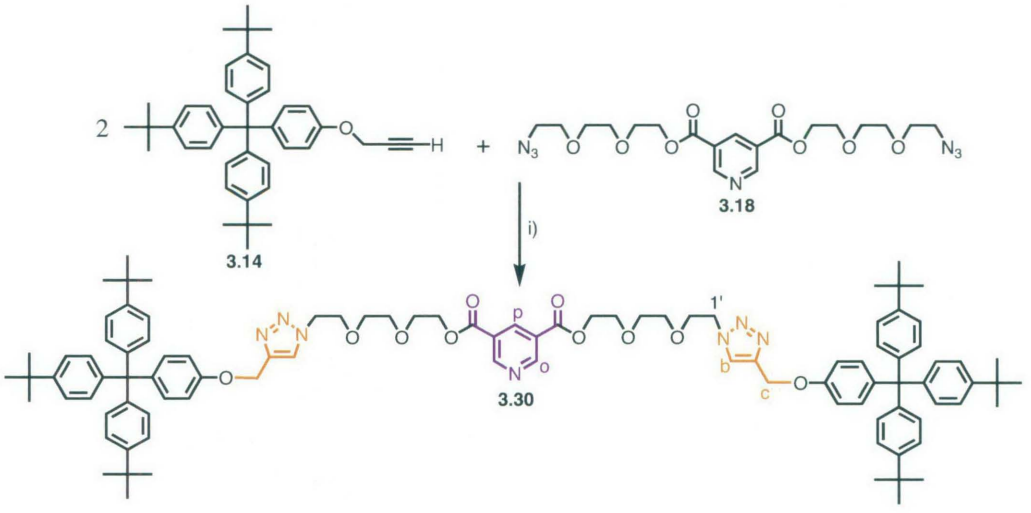

Scheme 3.12:- Reagents and conditions for the synthesis of pyridine dumbbell **3.30**; i) $Cu(MeCN)_4BF_4$, DIPEA, Toluene, 3 days RT, 70%.

After 3 days, the reaction produced the dumbbell **3.30** in reasonable yields. ^{1}H NMR analysis of the dumbbell showed the characteristic chemical shifts for the triazole protons b (7.80 ppm) and c (5.19 ppm). The pyridine protons o and p appeared at their characteristic uncoordinated positions of 9.40 and 8.89 ppm respectively. These chemical

shifts are consistent with similar triazole-containing dumbbells and molecules previously discussed.

Thus, having established the protocol for pyridine dumbbell synthesis using the click reaction, the reaction was attempted again in the presence of rhodium chloride strapped porphyrin **3.5**. As discussed previously this particular rhodium porphyrin derivative was chosen, as derivatives of pyridine thread **3.18** have shown preferential "inside" coordination for up to three days.

The ^{1}H NMR of the major rhodium porphyrin product showed clear resonances for bound pyridine protons at 6.09 and 1.74 ppm and the expected integration for a 1:1 complex between rhodium porphyrin macrocycle **3.5** and pyridine dumbbell **3.30**. However split *meso* protons at 10.29 and 9.88 ppm, as well as split hexyl and methyl side chains were evident, which is not expected in a rotaxane conformation. Furthermore only one set of peaks for the strapped porphyrin naphthalene aromatic protons (7.01, 6.18 and 5.25 ppm) were evident. These patterns in the strapped porphyrin protons is not consistent with a rotaxane structure, but rather with one in which central pyridine is coordinated on the same side of the porphyrin as the strap, but is not interlocked through the cavity, as seen in previous studies involving rotaxane formation *via* acid chloride reactions (See Section 3.4) and those involving coordination of bulky ligands to these strapped porphyrins (See Chapter 2, Section 2.4).

Furthermore, addition of pyridine to this complex showed complete dissociation of the dumbbell **3.30** from the rhodium porphyrin due to the stronger ligand pyridine coordinating to the rhodium porphyrin. This indicates that the two components are indeed *not* mechanically linked as a rotaxane, but that the product is simply a strongly coordinatively bound complex. Furthermore these two components (those being the free dumbbell and the rhodium-pyridine complex) could be separated by preparative TLC, confirming without a doubt that this mixture was not rotaxane. Similar problems were encountered in the acid chloride reactions discussed in Section 3.4, indicating that despite the milder reaction conditions and different stopper groups, folding of the flexible strap of

the porphyrin which in turn decreases the likelihood of interlocked molecules is still a problem.

Having ruled out rotaxane synthesis as an option to produce an interlocked species using pyridine templating with the added potential for "switching", attention was turned to catenane synthesis, as this negates the problematic folding of the strap due to possible π–π stacking interactions with large aromatic stopper groups. Two "click" reactions were set up involving the pyridine thread **3.18** and the diimide alkyne **3.19** with one reaction containing the rhodium chloride porphyrin **3.5** as the macrocycle in the hope that the pyridine ligand would template the reaction, whilst the other reaction contained the zinc porphyrin **3.2** which may produce catenane using either the diimide as the template or possibly the weak pyridine-zinc interaction (see Scheme 3.13).

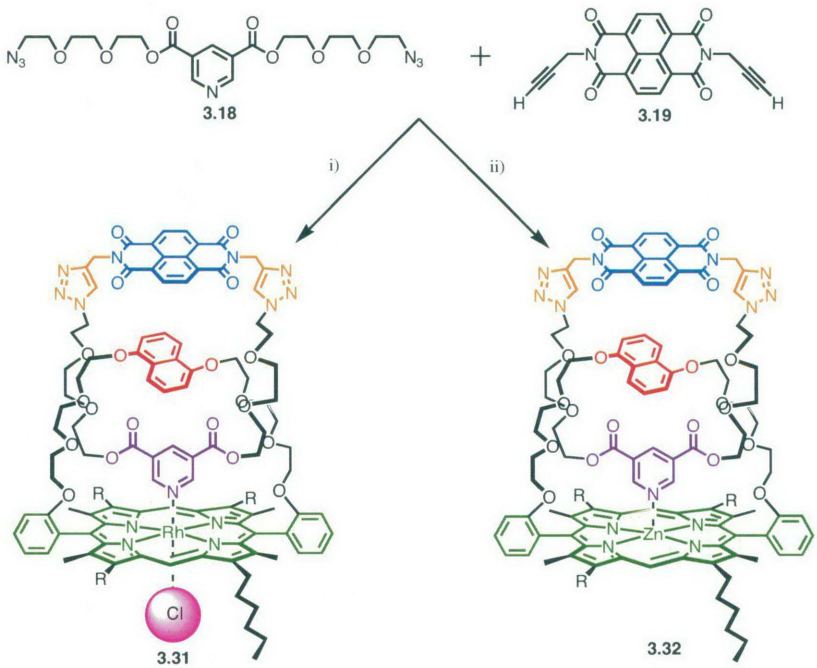

Scheme 3.13:- Reagents and conditions for the synthesis of catenanes **3.31** and **3.32**; i) porphyrin **3.5**, $Cu(MeCN)_4BF_4$, DIPEA, toluene, 4 days RT; ii) **3.2**, $Cu(MeCN)_4BF_4$, DIPEA, toluene, 4 days RT.

After 4 days, stirring under nitrogen at room temperature, visible white precipitate had formed in both reaction mixtures suggesting the reaction had progressed, however no catenane material was isolated in the subsequent workup of the reaction mixture. This solid produced was insoluble in all solvents and was thought to be due to polymeric material from the linear reaction between the pyridine and diimide threads. In both cases

all starting porphyrin material was recovered and no traces of catenane was observed. However time prevented a more detailed investigation into the use of "click" reactions to produce catenanes and hence no optimisation of the reaction conditions was performed. It is thought that changes in the concentration or temperature conditions under which the reactions are conducted may enable catenanes to be produced *via* this method. This must await future research.

3.7 SUMMARY AND CONCLUSIONS

Unfortunately the pyridine directed template synthesis of supramolecular systems incorporating strapped porphyrin macrocycles has proved problematic. Despite optimising conditions to increase the binding of such difunctionalised pyridine ligands used in this study, and optimising conditions such that the ligands were bound preferentially "inside" the strap of the porphyrin, attempts to produce rotaxanes and catenanes using a variety of reaction conditions proved problematic. Although the use of rhodium metalloporphyrins aided in the binding of pyridine ligands, competititive binding of common reagents used in catenane and rotaxane synthesis, such as EDC and triethylamine, inhibited some reactions. More frustratingly, the conditions that were suitable for rotaxane formation using the pyridine templating, resulted in the folding of the strap of the porphyrin, again negating the possibility of rotaxane formation.

Despite this, the use of the relatively new Cu(I) catalysed Huisgen 1,3-dipolar cycloaddition ("click" chemistry), produced not only numerous dumbbell components, but also two rotaxanes (one incorporating the crown host, and the other a strapped porphyrin macrocycle) in relatively good yields. Of particular interest is the strapped porphyrin rotaxane, which is the first successful rotaxane incorporating this host and the diimide guest. In this rotaxane, the diimide unit is preferentially bound underneath the strap of the porphyrin. However upon insertion of rhodium iodide (III) into the porphyrin the rotaxane "switched" so that the triazole entities were now coordinated to the Rh(III) ion underneath the strap, and the diimide was displaced from the cavity. Unfortunately this is not reversible, and no conditions were found that could create controlled, reversible "switching" for this rotaxane.

Nevertheless, this work has opened up numerous avenues of research to be continued. This type of 'click" chemistry shows great potential, and although preliminary catenation studies were performed much work is needed to optimise these reaction conditions allowing catenanes as well as rotaxanes to be isolated. Furthermore as the attempts to produce rotaxanes and catenanes involving the difunctionalised pyridine ligand were not successful, attention should be turned to find alternatively substituted ligands for similar work. Ideally an appropriately substituted pyridine ligand that coordinates relatively strongly to zinc metalloporphyrins should be investigated to avoid any problems associated with competitive binding of reagents such as triethylamine and EDC. It may also allow milder conditions for any future "switching" experiments, as zinc is easier to insert, and remove from porphyrins than metals such as rhodium or ruthenium. Hopefully, these aspects can be addressed by future research.

REFERENCES

(1) Vignon, S. A.; Jarrosson, T.; Iijima, T.; Tseng, H. R.; Sanders, J. K. M.; Stoddart, J. F., *J. Am. Chem. Soc.* **2004**, *126*, 9884-9885; Loeb, S. J., *Chem. Soc. Rev.* **2007**, *36*, 226-235; Elizarov, A. M.; Chiu, S. H.; Stoddart, J. F., *J. Org. Chem.* **2002**, *67*, 9175-9181; Martinez-Díaz, M.-V.; Spencer, N.; Stoddart, J. F., *Angew. Chem. Int. Ed.* **1997**, *36*, 1904-1907; Ashton, P. R.; Ballardini, R.; Balzani, V.; Fyfe, M. C. T.; Gandolfi, M. T.; Martínez-Díaz, M.-V.; Morosini, M.; Schiavo, C.; Shibata, K.; Stoddart, J. F.; White, A. J. P.; Williams, D. J., *Chem. Eur. J.* **1998**, *4*, 2332-2341; Ashton, P. R.; Ballardini, R.; Balzani, V.; Baxter, I.; Credi, A.; Fyfe, M. C. T.; Gandolfi, M. T.; Gomez-Lopez, M.; Martinez-Diaz, M.-V.; Piersanti, A.; Spencer, N.; Stoddart, J. F.; Venturi, M.; White, A. J. P.; Williams, D. J., *J. Am. Chem. Soc.* **1998**, *120*, 11932-11942; Ashton, P. R.; Baldoni, V.; Balzani, V.; Credi, A.; Hoffmann, H. D. A.; Martinez-Diaz, M.-V.; Raymo, F. M.; Stoddart, J. F.; Venturi, M., *Chem. Eur. J.* **2001**, *7*, 3482-3493.

(2) Tian, H.; Wang, Q.-C., *Chem. Soc. Rev.* **2006**, *35*, 361 - 374; Tseng, H.-R.; Vignon, S. A.; Celestre, P. C.; Perkins, J.; Jeppesen, J. O.; Fabio, A. D.; Ballardini, R.; Gandolfi, M. T.; Venturi, M.; Balzani, V.; Stoddart, J. F., *Chem. Eur. J.* **2004**, *10*, 155-172; Alteri, A.; Gatti, F. G.; Kay, E. R.; Leigh, D. A.; Martel, D.; Paolucci, F.; Slawin, A. M. Z.; Wong, J. K. Y., *J. Am. Chem. Soc.* **2003**, *125*, 8644-8654.

(3) Kay, E. R.; Leigh, D. A.; Zerbetto, F., *Angew. Chem. Int. Ed.* **2007**, *46*, 72-191; Balzani, V.; Credi, A.; Silvi, S.; Venturi, M., *Chem. Soc. Rev.* **2006**, *35*, 1135-1149.

(4) Gunter, M. J., *Eur. J. Org. Chem.* **2004**, 1655-1673.

(5) Flamigni, L.; Johnston, M. R., *New J. Chem.* **2001**, *25*, 1368-1370; Abraham, W.; Grubert, L.; Grummt, U. W.; Buck, K., *Chem. Eur. J.* **2004**, *10*, 3562-3568; Saha, S.; Stoddart, J. F., *Chem. Soc. Rev.* **2007**, *36*, 77-92; Qu, D.-H.; Wang, Q.-C.; Tian, H., *Org. Lett.* **2004**, *6*, 2085-2088.

(6) Gunter, M. J.; Farquhar, S. M., *Org. Biomol. Chem.* **2003**, *1*, 3450 - 3457.

(7) Hansen, J. G.; Feeder, N.; Hamilton, D. G.; Gunter, M. J.; Becher, J.; Sanders, J. K. M., *Org. Lett.* **2000**, *2*, 449-452.

(8) Bock, V. D.; Hiemstra, H.; van Maarseveen, J. H., *Eur. J. Org. Chem.* **2006**, *2006*, 51-68; Kolb, H. C.; Finn, M. G.; Sharpless, K. B., *Angew. Chem. Int. Ed.* **2001**, *40*, 2004-2021.

(9) Ball, P., *Chemistry World* **2007**, *4*, 46-51.

(10) Aucagne, V.; Hanni, K. D.; Leigh, D. A.; Lusby, P. J.; Walker, D. B., *J. Am. Chem. Soc.* **2006**, *128*, 2186-2187.

(11) Dichtel, W. R.; Miljanic, O. S.; Spruell, J. M.; Heath, J. R.; Stoddart, J. F., *J. Am. Chem. Soc.* **2006**, *128*, 10388-10390.

(12) Miljanic, O. S.; Dichtel, W. R.; Mortezaei, S.; Stoddart, J. F., *Org. Lett.* **2006**, *8*, 4835-4838.

(13) Trabolsi, A.; Elhabiri, M.; Urbani, M.; Delgado de la Cruz, J. L.; Ajamaa, F.; Solladie, N.; Albrecht-Gary, A. M.; Nierengarten, J. F., *Chem. Comm.* **2005**, 5736-5738; Hahn, U.; Elhabiri, M.; Trabolsi, A.; Herschbach, H.; Leize, E.; Dorsselaer, A. V.; Albrecht-Gary, A. M.; Nierengarten, J. F., *Angew. Chem. Int. Ed.* **1005**, *44*, 5338-5341; Ornelas, C.; Aranzaes, J. R.; Coutet, E.; Alves, S.; Astruc, D., *Angew. Chem. Int. Ed.* **2007**, *46*, 872-877; Ryu, E. H.; Zhao, Y., *Org. Lett.* **2005**, *7*, 1035-1037.

(14) Aprahamian, I.; Dichtel, W. R.; Ikeda, T.; Heath, J. R.; Stoddart, J. F., *Org. Lett.* **2007**, *9*, 1287-1290.

(15) Hamilton, D. G.; Davies, J. E.; Prodi, L.; Sanders, J. K. M., *Chem. Eur. J.* **1998**, *4*, 608-620.

(16) Ashton, P. R.; Ballardini, R.; Balzani, V.; Belohradsky, M.; Gandolfi, M. T.; Philp, D.; Prodi, L.; Raymo, F. M.; Reddington, M. V.; Spencer, N.; Stoddart, J. F.; Venturi, M.; Williams, D. J., *J. Am. Chem. Soc.* **1996**, *118*, 4931-4951.

(17) Hamilton, D. G.; Feeder, N.; Teat, S. J.; Sanders, J. K. M., *New J. Chem.* **1998**, 1019-1021.

(18) Sanders, J. K. M.; Wietor, J. L., *personal communications* in 2007.

(19) Zhang, Q.; Hamilton, D. G.; Feeder, N.; Teat, S. J.; Goodman, J. M.; Sanders, J. K. M., *New J. Chem.* **1999**, *23*, 897-903.

(20) Johnston, A. G.; Leigh, D. A.; Nezhat, L.; Smart, J. P.; Deegan, M. D., *Angew. Chem. Int. Ed.* **1995**, *34(11)*, 1212-1216.

(21) Gunter, M. J.; Bampos, N.; Johnstone, K. D.; Sanders, J. K. M., *New J. Chem.* **2001**, *25*, 166-173.

(22) Hamilton, D. G.; Montalti, M.; Prodi, L.; Fontani, M.; Zanello, P.; Sanders, J. K. M., *Chem. Eur. J.* **2000**, *6*, 608-617.

(23) Suijkerbuijk, B. M. J. M.; Aerts, B. N. H.; Dijkstra, H. P.; Lutz, M.; Spek, A. L.; van Koten, G.; Gebbink, R. J. M. K., *J. Chem. Soc., Dalton Trans.* **2007**, 1273-1276.

(24) Gunter, M. J.; Farquhar, S. M.; Jeynes, T. P., *Org. Biomol. Chem.* **2003**, *1*, 4097 - 4112; Gunter, M. J.; Hockless, D. C. R.; Johnston, M. R.; Skelton, B. W.; White, A. H., *J. Am. Chem. Soc.* **1994**, *116*, 4810-4823.

(25) Kim, H. J.; Redman, J. E.; Nakash, M.; Feeder, N.; Teat, S. J.; Sanders, J. K. M., *Inorg. Chem.* **1999**, *38*, 5178-5183.